2 1978

United States Environmental Protection Agency
Industrial Environmental Research Laboratory Research Triangle Park NC 27711
EPA-600/7-78-129
July 1978

EPA

Evaluation of Electrostatic Precipitator During SRC Combustion Tests

COPIED
OFFICIAL

Interagency Energy/Environment R&D Program Report

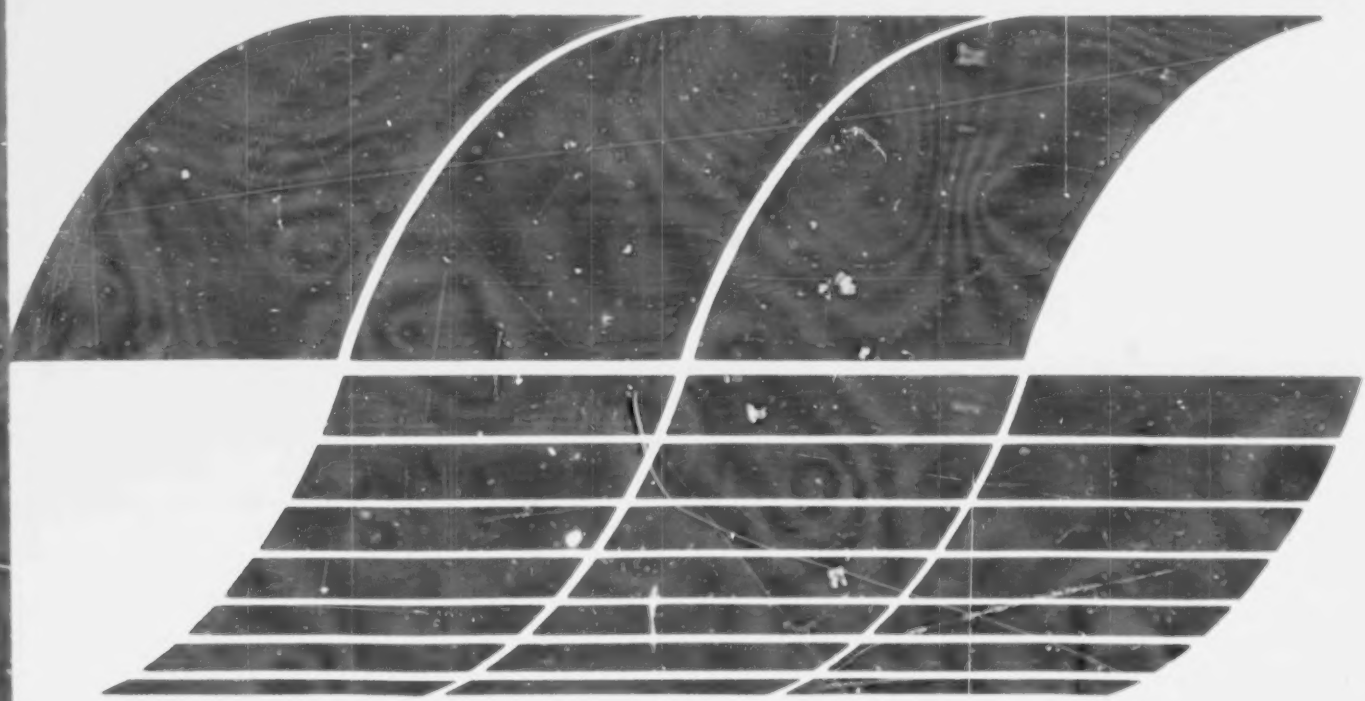

RESEARCH REPORTING SERIES

Research reports of the Office of Research and Development, U.S. Environmental Protection Agency, have been grouped into nine series. These nine broad categories were established to facilitate further development and application of environmental technology. Elimination of traditional grouping was consciously planned to foster technology transfer and a maximum interface in related fields. The nine series are:

1. Environmental Health Effects Research
2. Environmental Protection Technology
3. Ecological Research
4. Environmental Monitoring
5. Socioeconomic Environmental Studies
6. Scientific and Technical Assessment Reports (STAR)
7. Interagency Energy-Environment Research and Development
8. "Special" Reports
9. Miscellaneous Reports

This report has been assigned to the INTERAGENCY ENERGY-ENVIRONMENT RESEARCH AND DEVELOPMENT series. Reports in this series result from the effort funded under the 17-agency Federal Energy/Environment Research and Development Program. These studies relate to EPA's mission to protect the public health and welfare from adverse effects of pollutants associated with energy systems. The goal of the Program is to assure the rapid development of domestic energy supplies in an environmentally-compatible manner by providing the necessary environmental data and control technology. Investigations include analyses of the transport of energy-related pollutants and their health and ecological effects; assessments of, and development of, control technologies for energy systems; and integrated assessments of a wide range of energy-related environmental issues.

REVIEW NOTICE

This report has been reviewed by the participating Federal Agencies, and approved for publication. Approval does not signify that the contents necessarily reflect the views and policies of the Government, nor does mention of trade names or commercial products constitute endorsement or recommendation for use.

This document is available to the public through the National Technical Information Service, Springfield, Virginia 22161.

EPA-600/7-78-129
July 1978

Evaluation of Electrostatic Precipitator During SRC Combustion Tests

by

Grady B. Nichols and William J. Barrett

Southern Research Institute
2000 Ninth Avenue, South
Birmingham, Alabama 35205

Contract No. 68-02-2610
Task No. 2
Program Element No. EHE623A

EPA Project Officer: William J. Rhodes

Industrial Environmental Research Laboratory
Office of Energy, Minerals, and Industry
Research Triangle Park, NC 27711

Prepared for

US. ENVIRONMENTAL PROTECTION AGENCY
Office of Research and Development
Washington, DC 20460

FIGURES

Number		Page
1.	Electrostatic precipitator flowsheet—Georgia Power Company, Plant Mitchell	6
2.	ESP No. 1—Georgia Power Company, Plant Mitchell	8
3.	ESP No. 3—Georgia Power Company, Plant Mitchell	11
4.	Voltage versus current for a precipitator with 23-cm plate spacing and 0.25-cm corona wire	19
5.	Point-to-plane resistivity probes equipped for thickness measurement	21
6.	Typical voltage-current relationships for point-to-plane resistivity probe	22
7.	Voltage-current curves. Plant Mitchell full load coal Phase I, 1/25/77, Test 1	25
8.	Voltage-current curves. Plant Mitchell full load coal Phase I, 1/25/77, Test 2	26
9.	Electrical equivalent circuit of a precipitator electrode system with a dust layer	29
10.	Voltage-current relationship in an ideal capacitor resistor parallel combination	30
11.	Voltage divider network for measuring precipitator secondary voltages	32
12.	Sample V-I curve data sheet	33
13.	Voltage-current curves. ESP No. 1 full load coal 5/24/77—In A1 and Out A1. ESP No. 1 full load SRC 6/22/77—In A4 and Out A4	36

FIGURES (Concluded)

Number		Page
14.	Voltage-current curves. ESP No. 3 full load coal 6/8/77—In A3 and Out A3. ESP No. 3 full load SRC 6/22/77—In A5 and Out A5	37
15.	Voltage waveforms applied to the precipitators at Plant Mitchell	39

TABLES

Number		Page
1.	Electrostatic Precipitator Performance Data	12
2.	Resistivity Data—Phase II Tests	27
3.	Average Resistivities—Plant Mitchell Phase II	27
4.	Data from Runs with Regular Coal (Phase II)	43
5.	Data from Runs with Solvent Refined Coal (Phase III)	45

SECTION 1

INTRODUCTION

This report deals with the evaluation of an electrostatic precipitator (ESP) and associated environmental factors during the burning of solvent refined coal (SRC) in a boiler at Plant Mitchell of the Georgia Power Company. The tests described in this report were conducted during May and June 1977.

This effort was a part of an overall study of the use of solvent refined coal in a full-scale electric power plant. The study was sponsored by the U. S. Energy Research and Development Administration and the U. S. Environmental Protection Agency with the assistance of several contractors and subcontractors. The part of the overall study covered in this report was performed under Work Assignment No. 2 of Environmental Protection Agency Contract No. 68-02-2610 with Southern Research Institute. Under a subcontract with Southern Research Institute, York Research Corporation obtained plant operating data during the burning of unrefined coal (Phase I and Phase II) and later during the burning of solvent refined coal (Phase III). These data were analyzed and interpreted by Rust Engineering Company under another subcontract, with the assistance of Southern Research Institute personnel.

Institute personnel also collected various samples during Phase II and Phase III with a Source Assessment Sampling System (SASS train). These samples were delivered to Hittman Associates, who had an assignment to perform analyses for organic and inorganic emissions under another Environmental Protection Agency contract.

This report consists of three principal parts. The first part deals with the performance of the electrostatic precipitator system and was prepared by Rust Engineering Company. The second, closely associated part is concerned with the electrical resistivity of the fly ash and was prepared by Southern Research Institute. The third part describes the collection of samples for chemical analysis, and includes some comments on the operation of the SASS train.

SECTION 2

CONCLUSIONS AND RECOMMENDATIONS

The data on electrostatic precipitator performance were inconsistent and inconclusive, suggesting operational abnormalities that were not revealed by the test data. In particular, the performance of the precipitator was abnormal during baseline firing with unrefined coal. The data were not adequate to define the design parameters for an electrostatic precipitator operating at an SRC-fired boiler. The high carbon content, low electrical resistivity, and low bulk density of the SRC particulate emissions, in conjunction with operational factors such as gas velocities and plate electrode areas, appeared to be associated with the low observed collection efficiency. It is recommended that additional test programs be performed to define more accurately the behavior of a precipitator collecting particulate emissions from the burning of solvent refined coal.

Even though there are potential problems with the test data developed in this program, one could expect an electrostatic precipitator to behave at least as well as ESP No. 3 under normal conditions.* One would expect a new precipitator, designed with a specific collection electrode area of about 1.3 $m^2/m^3/min$ (400 $ft^2/1000\ ft^3/min$) and a gas velocity of about 0.6 m/sec (2 ft/sec) to attain a collection efficiency of about 95% with an outlet mass loading of about 0.05 g/m^3 (0.02 gr/scf) as given by tests 32 through 34 of Table 1.

The question of the need for additional tests is based on the need to better define the required rapping and gas flow characteristics for an electrostatic precipitator installed in a new solvent refined coal boiler. This additional test could perhaps be conducted in a pilot-scale operation rather than a full size boiler because of the limited amount of solvent refined coal available for additional tests.

---

* See Figure 1 on page 6 and the text on page 10 for descriptions of the emission control system and ESP No. 3.

No major difficulties were encountered in the operation of the SASS train. However, the small particle size and possibly the carbonaceous nature of the SRC particulate emissions resulted in rapid clogging of the filters, necessitating frequent filter changes. This minor problem might be alleviated by the use of larger filters, with redesign of the oven to provide more space for the cyclone-filter assembly.

SECTION 3*

PERFORMANCE OF THE ELECTROSTATIC PRECIPITATOR SYSTEM

INTRODUCTION

The Rust Engineering Company participated in a program designed for the evaluation of operating parameters in a full-scale commercial steam generating unit when fired with a fuel consisting of solvent refined coal.

The program was directed and managed by Southern Company Services, Inc., the engineering and research subsidiary of the Southern Company, Atlanta, Georgia, a public utility holding company whose operating subsidiaries include Georgia Power Company, Alabama Power Company, Gulf Power Company, Mississippi Power Company, and Southern Electric Generating Company. The test burn was sponsored by the US Energy Research and Development Administration. The ESP evaluation was sponsored by the US Environmental Protection Agency. Other participating companies included:

The Babcock and Wilcox Company
Southern Research Institute
York Research Corporation
The Pittsburgh & Midway Coal Mining Company
Hittman Associates, Inc.
Battelle Northwest
TRW Systems and Energy
Bechtel Corporation
Wheelabrator-Frye, Inc.

The test program was performed in various stages between January and June 1977. This report pertains to the part of the program concerned with the evaluation of the performance of the electrostatic precipitation system, installed for the removal of solid particulate matter from the exhaust gases emanating from the test boiler.

---

* Section 3 was prepared by John E. Paul, Senior Staff Engineer, Rust Engineering Company.

PLANT DESCRIPTION

The test program was conducted at the Mitchell Power Station of the Georgia Power Company, an operating subsidiary of the Southern Company, Atlanta, Georgia. The plant is located on State Highway 3, south of Albany, Georgia.

The test unit is identified as Boiler No. 1, a 22.5-MW rated B & W boiler, fired with pulverized fuel. The boiler is equipped with three B & W coal mills, front-wall burner arrangement, and features in its exhaust gas path a Ljungstrom-type air preheater, a primary electrostatic precipitator (Research Cottrell, Inc.) identified as ESP No. 1, an induced draft (ID) fan, and a secondary electrostatic precipitator (American Standard), identified as ESP No. 3. ESP No. 3 serves to clean the combined exhaust gases emanating from No. 1 and No. 2 Boilers (see Figure 1).

TEST PROGRAM

The test program was divided into three phases:

Phase I: Baseline data acquisition.
Test boiler operation with conventional burners on normal coal.

Phase II: Baseline data acquisition.
Test boiler operation with modified burners on normal coal.

Phase III: Test data acquisition.
Test boiler operation with modified burners and readjusted fuel mills on solvent refined coal.

Each phase included boiler operation at rated full load, two-thirds load, and one-third of full load. Data acquisition included:

1. Pulverizer (mill) performance.
2. Boiler performance.
3. Fuel handling equipment.
4. Combustion performance.
5. Particulate mass loading in exhaust gases (ASME and EPA Method 5 tests).
    a. Upstream of ESP No. 1.

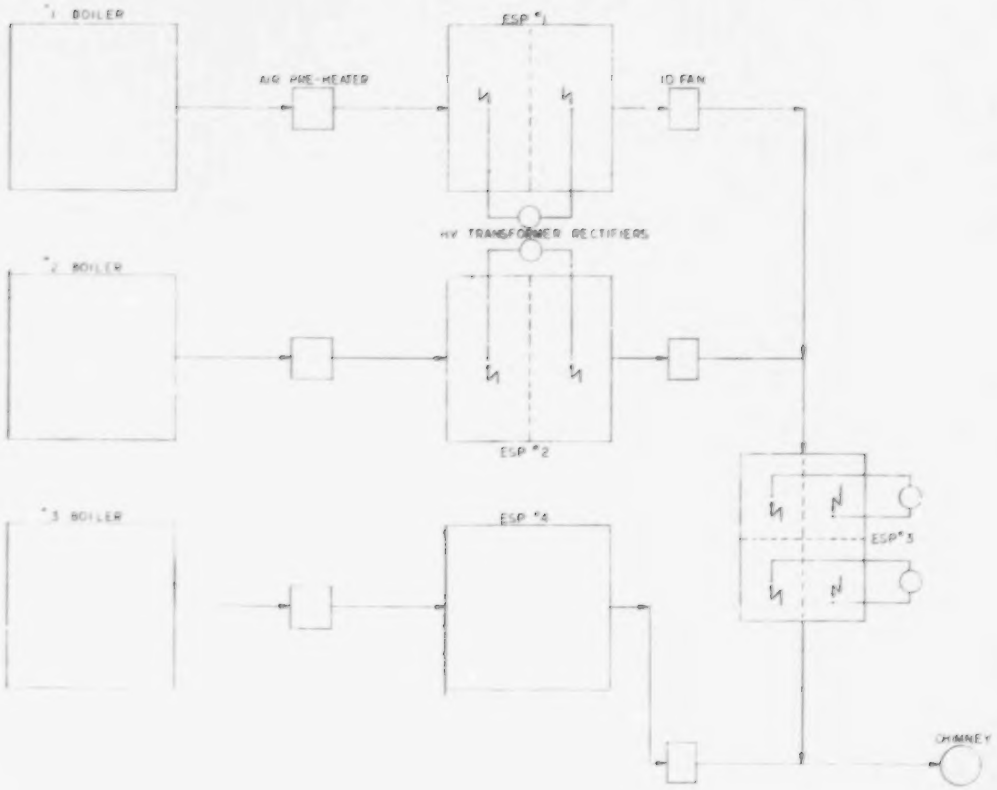

Figure 1. Electrostatic precipitator flowsheet — Georgia Power Company, Plant Mitchell.

b. Downstream of ESP No. 1.

c. Downstream of ESP No. 3.

6. Particulate sizing, same locations as 5.

7 Exhaust gas analysis for O_2, CO, and CO_2.

8. SO_2 concentration.

9. NO_x concentration.

10. Hydrocarbon concentration.

11. Chemical analysis of fuel, bottom ash, and fly ash.

12. Electrical resistivity of fly ash.

13. Precipitation current and V/I relationship.

ELECTROSTATIC PRECIPITATORS

Description of ESP No. 1

ESP No. 1 is of Research Cottrell, Inc. (RC), design and was put into operation in 1947. It is of the horizontal gas flow type, generally as shown in Figure 2.

The precipitator consists of one chamber having two independent electrical fields in series, which were originally energized by high voltage (HV) transformers with mechanical, synchronous motor driven rectifiers. High voltage cables are used for power transmission.

Several years ago the mechanical rectifiers were replaced with new solid state rectifiers housed integrally with the transformers and provided with modern saturable core reactor voltage control equipment.

One HV energizing unit supplies the required precipitation power to both inlet and outlet fields via a double half-wave bridge rectifier arrangement. Voltage control upon input signal based on spark rate limitation, dc current, or voltage limitation thus affects both fields.

The precipitator is equipped with collecting electrodes made of expanded metal sheets tied together by anvil bars at the front and rear ends and suspended from structural members located in the roof structure. Discharge electrodes are single round wires of 0.25 cm (0.1 in.) diameter, suspended from a framework located between fields, and supported from bushing type ceramic insulators

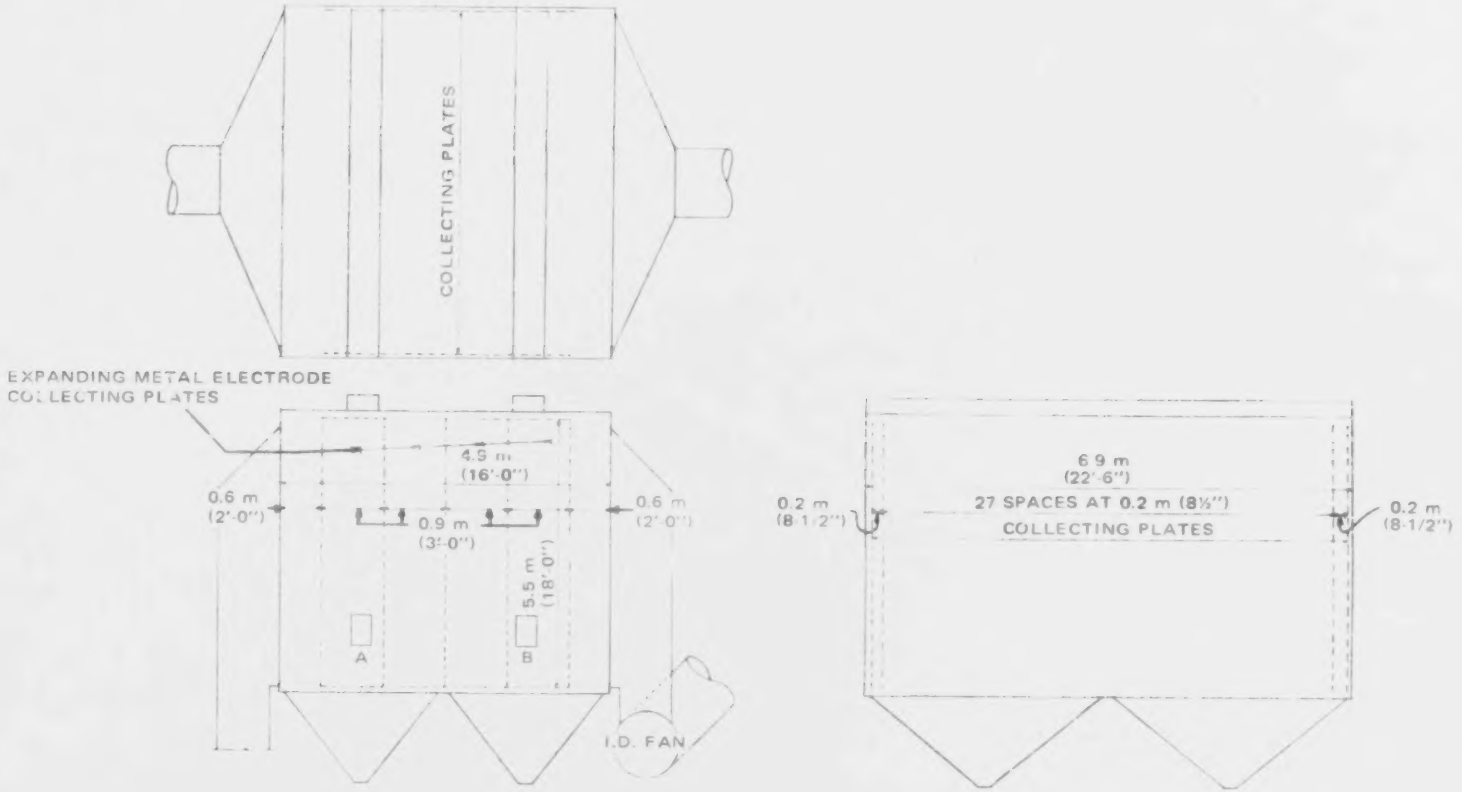

Figure 2. ESP No 1 – Georgia Power Company, Plant Mitchell.

in the roof-mounted insulator compartment. These wires are held in plumb suspension between collecting electrodes by weights fastened to their lower extremities.

Collecting electrode (CE) plates are cleaned by side-wall mounted, solenoid-operated impact rappers, acting horizontally and perpendicular to the plates and the gas stream, thus promoting thrust for reentrainment of collected material. No equipment is provided for discharge electrode (DE) cleaning.

The precipitator is equipped with perforated gas velocity distribution plates located in the inlet and outlet plenum.

Field measurements and Research Cottrell supplied design information are as follows:

Design gas volume	4800 m^3/min (170,000 ACFM)
Design gas temperature	175°C (350°F)
Design efficiency	90%
CE area (effective)	963 m^2 (10,368 ft^2)
DE length	2960 m (9,720 ft)
Design specific collecting area (SCA)	12 m^2/m^3/sec (61 ft^2/1000 ACFM)
Free face opening	25.8 m^2 (277.6 ft^2)
Design treatment velocity	3.1 m/sec (10.2 ft/sec)
CE height	5.5 m (18 ft)
Number of CE plates	28
CE length (two plates in each of two fields)	1.8 m (6 ft)/field
Total effective treatment length	3.66 m (12 ft)
Design treatment time	1.3 sec
CE spacing	20 cm (8 in.)

The precipitator was inspected during the week of January 17, 1977. The following comments apply.

The internal components of the precipitator were found to be in excellent condition. Specifically, there were no broken or

missing discharge electrode wires, and no deterioration or corrosion of collecting electrodes. No excessive accumulation of ash was observed on collecting electrode surfaces and wires showed only isolated spots of ash buildup in the form of hardened enlargements up to 6 cm (2.5 in.) diameter. All insulators were found to be in good workable condition. High voltage cables are regularly topped with insulating liquid.

The perforated plates in the inlet were clean; there was some accumulation of ash on the outlet side.

The ideal alignment between discharge wires and collecting electrode surfaces would be 9.8 cm (3-7/8 in.); the worst alignment measured was 11.7 cm (4-5/8 in.) one side to 8.7 cm (3-7/16 in.) on the opposite side.

Prior to commencement of testing, the precipitator was thoroughly cleaned by plant personnel. This included inlet and outlet plenums and ductwork.

Description of ESP No. 3

ESP No. 3 is of American Standard design and was placed in service in 1962. It was originally installed to treat the gases exhausting from No. 3 Boiler, a 125-MW unit not a subject of this test series. The ducting to and from this ESP was later modified to provide for its operation on the combined gases from No. 1 and No. 2 Boilers.

The precipitator is of the horizontal gas flow type, generally as shown in Figure 3. The precipitator consists of two chambers, having two independent electrical fields in series, and it is energized by two HV transformer-rectifier power units with double half-wave bridge configuration and saturable core reactor voltage control equipment. The two discharge electrode bus systems in each chamber are energized each by one half-leg of the open electrically negative rectifier bridges, rated at 1,200 mA pulsating dc output. The total effective collecting electrode surface area has been measured at 4630 m^2 (49,882 ft^2).

A physical inspection of the precipitator revealed no discrepancies in discharge electrode or collecting electrode systems which would affect the normal performance of the equipment. Several high voltage support bushings showed hairline cracks. These bushings were exchanged for new bushings prior to commencement of testing.

TEST RESULTS

A summary of the relevant test data is presented in Table 1.

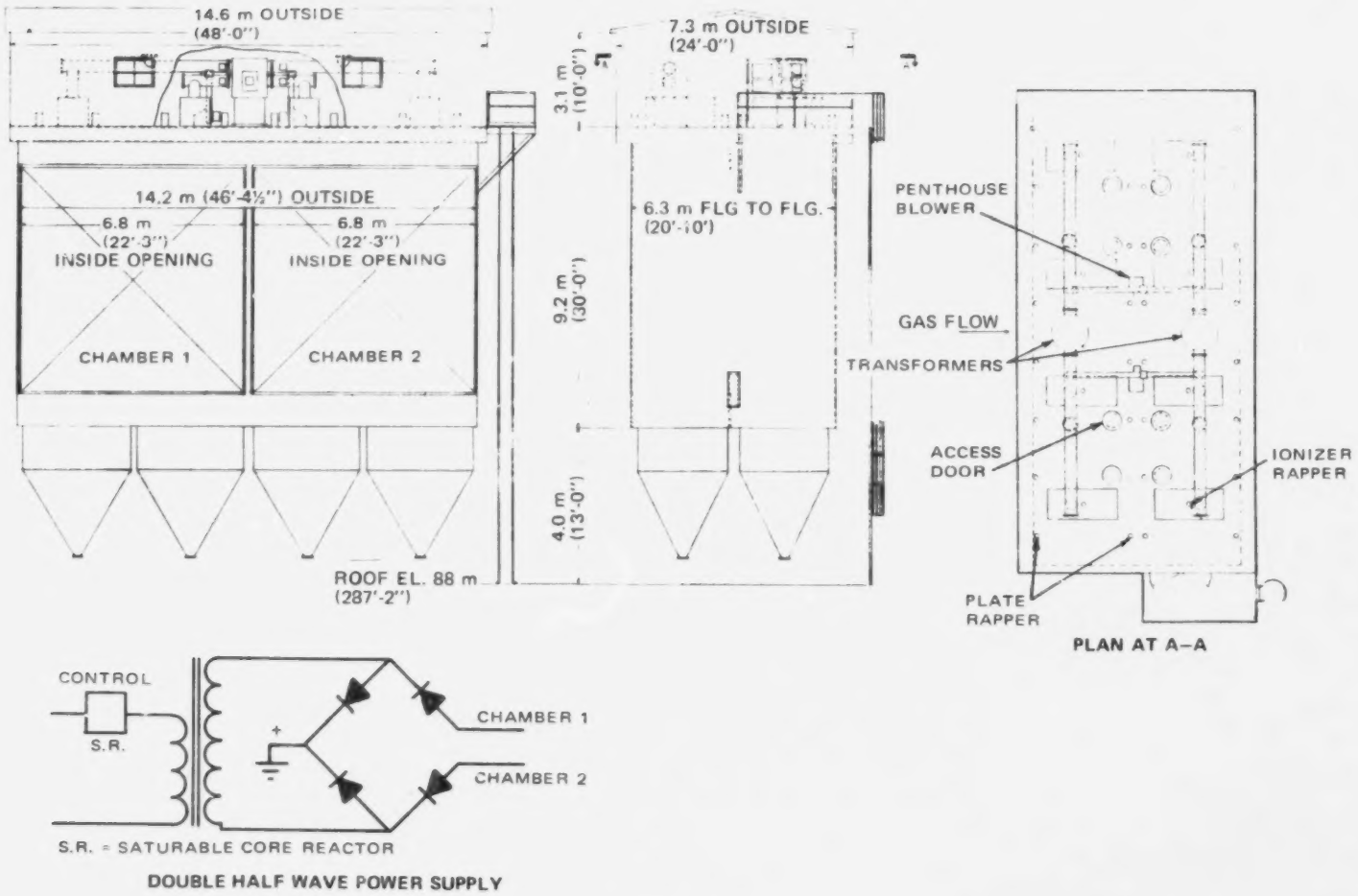

Figure 3. ESP No. 3 – Georgia Power Company, Plant Mitchell.

TABLE 1. ELECTROSTATIC PRECIPITATOR PERFORMANCE DATA

Parameter	Phase I Data (ESP No. 1) Test No. 1	2	3	4	5	6	7	8	9
Date	3/22	3/23	3/24	3/24	3/26	3/27	3/28	3/29	3/30
Boiler load, MW	22.5	22.5	15.0	7.5	7.5	7.5	22.5	15.0	15.0
Gas flow, ESP outlet, m^3/min	3656	3392	2493	1660	1595	1791	3497	2491	2565
Gas temp, °C	161	152	136	126	130	128	159	148	148
H_2O, %	4.0	6.2	6.0	6.9	5.4	5.4	6.0	8.4	6.8
Particulate concn, inlet, g/m^3 (dry)	9.21	8.86	8.85	6.75	6.78	6.27	10.66	9.00	10.73
Particulate concn, outlet, g/m^3 (dry)	2.64	1.78	0.45	0.06	0.07	0.08	2.11	0.23	0.41
Efficiency, %	71.3	79.9	94.9	99.1	99.0	98.7	80.2	97.4	96.2
Av power input, W/m^2	-	-	-	-	-	-	-	-	-
SCA, m^2/1000 m^3/min	263	283	386	580	604	538	275	387	376
W, calculated, cm/sec	7.912	9.420	12.884	13.599	12.763	13.437	9.800	15.775	14.532
Inlet dust, %									
1 µm	1.2	-	1.5	1.2	-	-	-	-	-
5 µm	20	-	10	14	-	-	-	-	-
10 µm	25	-	22	30	-	-	-	-	-
Fractional efficiency, %									
Smaller than 1 µm	15.0	-	12.0	78.0	-	-	-	-	-
Smaller than 5 µm	32.0	-	61.0	93.0	-	-	-	-	-
Smaller than 10 µm	48.0	-	80.0	95.0	-	-	-	-	-
Boiler operating data									
C-burning efficiency, %	97.94	97.16	97.40	96.48	97.25	96.52	97.58	97.20	97.70
O_2, %	4.8	4.9	5.7	11.2	9.7	11.1	4.3	6.1	6.1
Fuel flow, kg/min	186	181	145	67	67	69	179	119	122
Air flow, kg/min	1700	1710	1330	937	960	1000	1750	1350	1350
C in ash, %	14.3	15.5	17.1	21.6	17.8	19.1	11.8	15.2	11.1

(Continued)

TABLE 1 (continued).

Parameter	Phase II Data (ESP No. 1 and ESP No. 3) Test No.*										
	10	11	13	14	15	16	17	18	19	20	21
ESP No.	1	1	1	1	1	1	1	1	3	3	3
Date	5/24	5/25	5/27	5/28	5/29	5/30	5/31	6/1	6/5	6/5	6/6
Boiler load, MW	21.0	14.0	21.0	21.0	14.0	14.0	7.5	7.5	21.0	21.0	21.0
Gas flow, ESP outlet, m^3/min	3687	3000	3755	3775	3201	3151	1806	1934	3320	3499	3420
Gas temp, °C	152	147	150	152	144	143	146	138	139	146	137
H_2O, %	6.7	6.2	5.9	7.4	6.1	6.1	6.2	5.6	7.0	6.6	6.9
Particulate concn, inlet, g/m^3 (dry)	9.14	9.96	5.70	4.54	3.02	6.58	4.94	6.05	4.02	3.74	4.40
Particulate concn, outlet, g/m^3 (dry)	1.66	0.52	1.29	1.32	0.40	0.82	0.11	0.28	0.09	0.03	0.06
Efficiency, %	81.8	94.8	77.4	70.9	86.8	87.5	97.8	95.4	97.8	99.2	98.6
Av power input, W/m^2	-	-	-	-	-	-	-	-	5.87	6.12	5.76
SCA, $m^2/1000\ m^3/min$	261	321	257	255	300	306	533	498	1394	1325	1355
W, calculated, cm/sec	10.884	15.367	9.641	8.022	11.221	11.339	11.826	10.268	4.519	5.896	5.251
Inlet dust, %											
1 µm	2.0	3.5	-	-	-	-	3.0	-	2.2	-	-
5 µm	24	18	-	-	-	-	30	-	20	-	-
10 µm	45	40	-	-	-	-	50	-	40	-	-
Fractional efficiency, %											
Smaller than 1 µm	49.4	74.8	-	-	-	-	85.5	-	-	-	-
Smaller than 5 µm	64.2	75.0	-	-	-	-	91.5	-	-	-	-
Smaller than 10 µm	68.6	82.6	-	-	-	-	93.1	-	-	-	-
Boiler operating data											
C-burning efficiency, %	98.34	96.36	97.77	97.94	-	-	-	-	97.93	98.32	97.62
O_2, %	4.5	6.5	4.2	4.1	6.0	6.3	11.6	11.6	4.6	4.6	4.7
Fuel flow, kg/min	169	116	160	151	106	115	71	73	152	150	152
Air flow, kg/min	1910	1490	1900	1900	1590	1600	1130	1150	1930	1900	1940
C in ash, %	9.5	16.2	18.7	21.5	22.8	22.7	16.9	16.8	30.0	25.1	29.1

* Test No. 12 on May 26 aborted because the fuel feeder tripped.

(Continued)

TABLE 1 (continued).

Parameter	Phase III Data (ESP No. 1 and ESP No. 3) Test No.* 22	23	24	25	26	27	28	29	31	32	33	34
ESP No.	1	1	1	1	1	1	1	1	3	3	3	3
Date	6/13	6/14	6/15	6/16	6/17	6/18	6/19	6/20	6/22	6/22	6/23	6/23
Boiler load, MW	21.0	14.0	7.5	21.0	21.0	7.5	7.5	14.0	21.0	21.0	21.0	21.0
Gas flow, ESP outlet, m^3/min	3609	3076	1947	3621	3629	2007	7005	3229	3282	3271	3328	3471
Gas temp, °C	161	144	151	166	160	147	147	147	153	157	148	152
H_2O, %	6.8	6.2	5.4	6.7	7.3	6.0	5.9	7.6	7.4	8.2	6.6	9.1
Particulate concn, inlet, g/m^3 (dry)	1.07	1.28	1.08	1.00	1.00	1.08	1.09	1.66	0.99	0.84	[illegible]	0.73
Particulate concn, outlet, g/m^3 (dry)	0.87	1.00	0.49	0.83	0.80	0.62	0.59	1.23	0.13†	0.03†	0.04‡	0.038
Efficiency, %	18.4	21.9	56.6	17.0	20.0	42.3	45.9	25.9	86.9	96.4	95.1	95.9
Av power input, W/m^3	-	-	-	-	-	-	-	-	5.19	6.07	7.35	7.37
SCA, m^2/1000 m^3/min	267	313	495	266	265	480	481	298	1410	1417	1391	1335
W, calculated, cm/sec	1.267	1.320	2.817	1.159	-	1.912	2.116	1.688	2.404	3.762	3.587	4.002
Inlet dust, %												
1 µm	4.0	5.0	4.2	-	-	-	-	-	6.0	-	-	-
5 µm	20	18	15	-	-	-	-	-	28	-	-	-
10 µm	30	22	22	-	-	-	-	-	40	-	-	-
Fractional efficiency, %												
Smaller than 1 µm	20.9	44.1	41.5	-	-	-	-	-	74.5	-	-	-
Smaller than 5 µm	-	-	17.8	-	-	-	-	-	83.8	-	-	-
Smaller than 10 µm	-	-	-	-	-	-	-	-	85.7	-	-	-
Boiler operating data												
C-burning efficiency, %	98.51	97.63	96.89	98.37	98.28	-	-	-	98.28	98.66	98.65	98.80
O_2, %	5.4	7.2	11.7	5.6	5.8	10.9	11.2	7.4	6.7	6.7	5.7	5.7
Fuel flow, kg/min	132	91	54	134	133	56	56	95	136	134	133	133
Air flow, kg/min	1880	1690	1120	1840	1860	1160	1130	1780	1880	1890	1960	1950
C in ash, %	75.7	88.5	89.7	82.4	84.8	88.9	89.7	86.0	80.5	77.0	75.0	66.3

* Test No. 30 on June 21 was aborted because of a change in load demand.

† The plate rapping cycle was 5 min (continuously sequential).

‡ The plate rapping cycle was 15 min (manually intermittent).

§ The plate rapping cycle was 25 min (manually intermittent).

Conversion factors for Table 1

To convert	to	multiply by
m^3/min	ACFM	35.314
g/m^3	gr/SCF	0.437
m^3/1000 m^3/min	ft^3/1000 ACFM	0.3048
W/m^2	W/ft^2	0.0929
kg/min	lb/hr	132.3

The low efficiencies obtained by ESP No. 1, the primary precipitator, during SRC firing reflects the difficulty of precipitating material of extremely low electrical resistivity. This was expected.

It was not expected, however, that ESP No. 3, the secondary precipitator, would operate at calculated migration velocities of only 2.5 to 4 cm/sec during SRC firing. Its subnormal performance at migration velocities of 4.5 to 5.2 cm/sec during full-load base coal firing is highly suspect of some operational abnormality, as yet not identified. A possible cause could be bad gas velocity distribution within the precipitator inter-electrode space.

Neither precipitation power input nor measured particle size distribution provide any explanation for the apparent performance discrepancy. It is possible that the size distribution measurements are subject to error not identifiable at this time.

The specific problems associated with interpreting the data from ESP No. 3 involve the uncertainties in particle size distribution provided during the short test period allocated to this collector. As stated previously, the exhaust gases from Boilers 1 and 2 are combined prior to introduction into this control device. In order to conduct measurements on the effluent from Boiler No. 1, Boiler No. 2 must be shut down. The shutdown of Boiler No. 2 resulted in a very low gas velocity through the collector—approximately 0.6 m/sec (1.9 ft/sec).

It is to be noted that the gas flow control turning vanes were designed for gas velocities of about 1.5 to 1.8 m/sec (5 to 6 ft/sec). Thus, it is not unreasonable to expect the gas velocity distribution to be more nonuniform when the gas comes from only one boiler.

A second factor of concern is the behavior of the control device when collecting the very high carbon content particulates. It is to be expected that the proper rapping conditions—acceleration and interval—for the solvent refined coal residue will be significantly different than for fly ash. The optimization of these factors was not attempted in this test period.

CONCLUSION AND RECOMMENDATION

The data available from this test program do not appear to be adequate to arrive at a definitive conclusion as to the sizing requirements for an electrostatic precipitation system operating at an SRC-fired boiler. If anything, the interpretation of the data would result in a very conservative design approach, pointing to an electrode surface area requirement of 80 to 120 m^2 (400 to

600 ft^2) of collecting electrode area per cubic meter per second (1000 ACFM) for an outlet loading of approximately 0.05 g/m^3 (0.02 gr/SCF).

Several items were mentioned above that could degrade the performance of the electrostatic precipitator. Therefore, one cannot state conclusively what the optimum design for a precipitator for the new SRC facility would be. One can, however, state that if the conditions used in this test were duplicated, then the new control device would be expected to operate at least as well as the performance observed in ESP No. 3 while collecting particulate from Boiler No. 1.

A word of caution is in order. The particulate that results from the combustion of solvent refined coal is a very low density material that is high in carbon content. This particulate closely resembles that from the combustion of fuel oil. This highly conductive material is especially susceptible to reentrainment. Therefore, the principles of design for electrostatic precipitators for oil-fired units should be applied to any new SRC plant. Specifically, special attention should be paid to attaining a near uniform gas velocity distribution and the face velocity through the electrostatic precipitator should be maintained at about 0.6 m/sec (2 ft/sec).

It is recommended to pursue additional test programs to define more accurately the behavior of an electrostatic precipitator collecting SRC dust.

The additional tests recommended for a further definition of the particulate and electrostatic precipitator parameters should center on determining the particle size distribution and gas velocity distribution. It is recognized that another full-scale SRC test is not practical at this time. Since the particle size distribution measurements are so critical to the design of a new control device, these data would be extremely useful. If an acceptable small-scale combustor could be located that would duplicate the time-temperature profile of the furnace as well as the particle size distribution, a pilot-scale evaluation could provide useful data. However, care must be exercised in the selection of the pilot-scale device. One possible candidate is the Babcock and Wilcox minicombustor.

A test that could provide useful data at Plant Mitchell is to determine the gas velocity distribution with ESP No. 3. This measurement would require a 2-day shutdown of Boilers 1 and 2 and hot wire anemometer measurements within the interelectrode space. We suggest that these measurements be considered.

SECTION 4*

ELECTRICAL RESISTIVITY OF THE FLY ASH

BACKGROUND

The electrical resistivity of particulate matter present in the effluent gas stream is one of the primary factors that determine the operating characteristics of an electrostatic precipitator. The following paragraphs excerpted from a report by Nichols[1] are reproduced here to provide an understanding of the importance of the resistivity determinations and the methods by which in situ resistivity was measured.

Significance of Particulate Resistivity to Electrostatic Precipitator Operation

In a conventional single-stage, dry-electrode electrostatic precipitator, the total corona current flows through the collected dust layer to reach the grounded collection electrode. This flow of current establishes an electric field (E) in the dust layer which is proportional to the corona current density (j) and the particulate resistivity (ρ) as given by

$$E = j\rho. \qquad (1)$$

The electric field in the dust layer yields a voltage drop (ΔV) across the dust layer which is proportional to the dust layer thickness (t) and is given by

$$\Delta V = Et. \qquad (2)$$

---

* This section was prepared by Sherman M. Banks, Electrical Engineer, and Dr. Jack R. McDonald, Head, Theoretical and Basic Studies Section, Southern Research Institute.

1. Nichols, Grady B. "Techniques for Measuring Fly Ash Resistivity", EPA Report No. 650/2-74-079, US Environmental Protection Agency, pp. 2-4.

If the resistivity of the dust layer is increased while the current density is held constant, the electric field in the layer increases proportionately (Equation 1). If the electric field in the dust layer exceeds the field strength for corona initiation (electrical breakdown), an electron avalanche will occur in the dust layer similar to that which occurs adjacent to the corona wire. This electrical breakdown acts as a limit on the allowable electrical conditions in the precipitator as is discussed below.

The manner in which this breakdown limits the precipitator performance is dependent upon the value of the resistivity of the dust and the thickness of the layer. If the resistivity is in the moderately high range ($\sim 10^{12}$ ohm-cm) breakdown of the dust layer will occur at a voltage too low to propagate a spark across the interelectrode region. This gives rise to a condition of reverse ionization or back corona. Figure 4 illustrates these two conditions. The figure shows the current density as a function of applied voltage for an electrostatic precipitator with a 0.28-cm (0.109-in.) diameter corona wire, a 23-cm (9-in.) plate spacing, and a dust layer thickness of 1 cm (0.5 in.). If the dust layer resistivity is in the moderately high range, e.g., 2×10^{11} ohm-cm, electrical breakdown in the dust layer will occur at an applied voltage greater than that required for sparking between clean electrodes, and sparking will occur at a reduced current density. For a very high resistivity dust with the conditions shown, electrical breakdown will occur in the dust layer at a much lower current density and applied voltage. Under these conditions, the dust layer will be continuously broken down electrically and will interject into the interelectrode space ions of an opposite electrical polarity from those produced by the corona. The precipitator electrical operating conditions are thus limited by a high resistivity dust layer and the precipitator is constrained to operate at lower currents and voltages than one collecting a lower resistivity dust. The magnitude of the reduction in electrical operating conditions is a direct function of the dust resistivity.

In view of the importance of the resistivity of the dust layer as a primary factor in limiting the performance of a precipitator, it becomes necessary to determine the resistivity of the material to be collected in order to estimate the conditions to be expected in a precipitator.[2]

---

2. White, H. J. "Resistivity Problems in Electrostatic Precipitation". J. Air Pollut. Control Assoc., 24 (4), April 1974, p. 316.

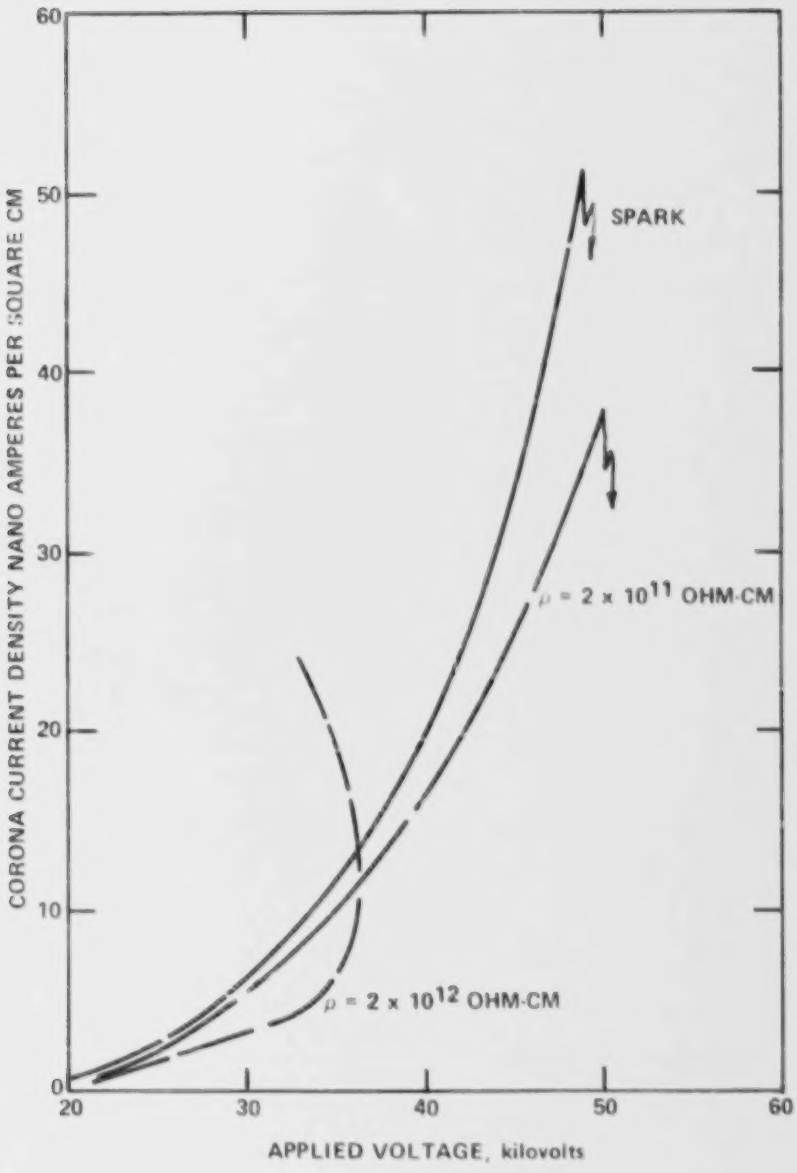

Figure 4. Voltage versus current for a precipitator with 23-cm plate spacing and 0.25-cm corona wire. Solid curve is for a clean electrode. The two dashed curves represent conditions for a 0.5-cm layer of dust with the resistivities indicated.

Point-to-Plane Probe

The point-to-plane probe for measuring resistivity has been in use since the early 1940's in this country.[2] Two models of this device are shown in Figure 5. The probe is inserted directly into the dust-laden gas stream and allowed to come to thermal equilibrium. The particulate sample is deposited electrically onto the measurement cell through the electrostatic action of the corona point and plate electrode. A high voltage is impressed across the point and plane electrode system such that a corona is formed in the vicinity of the point. The dust particles are charged by the ions and perhaps by free electrons from this corona in a manner analogous to that occurring in a precipitator.

The dust layer is formed through the interaction of the charged particulate with the electrostatic field adjacent to the collection plate. Thus, this device is intended to simulate the behavior of a full-scale electrostatic precipitator and to provide a realistic value for the resistivity of the dust that would be comparable to that in the actual device.

In the point-to-plane technique, two methods of making measurements on the same sample may be used. The first is the "V-I" method. In this method, a voltage-current curve is obtained before the electrostatic deposition of the dust, while the collecting disc is clean. A second voltage-current curve is obtained after the dust layer has been collected. After the layer has been collected and the clean and dirty voltage-current curves obtained, the second method of making a measurement may be used. In the second method, a disc the same size as the collecting disc is lowered on the collected sample. Increasing voltages are then applied to the dust layer and the current obtained is recorded until the dust layer breaks down electrically and sparkover occurs. The geometry of the dust sample, together with the applied voltage and current, provides sufficient information for determination of the dust resistivity.

In the point-to-plane method, the voltage drop across the dust layer is determined by the shift in the voltage-versus-current characteristics along the voltage axis as shown in Figure 6. The situation shown is for resistivity values ranging from 10^9 to 10^{11} ohm-cm.

If the parallel disc method is used, dust resistance is determined from the voltage measured just prior to sparkover. In both methods the resistivity is calculated as the ratio of the electric field to the current density.

The practice of measuring the resistivity with increasing voltage has evolved because the dust layer behaves as a nonlinear resistor. As the applied voltage is increased, the current increases greater than that attributable to the increase in

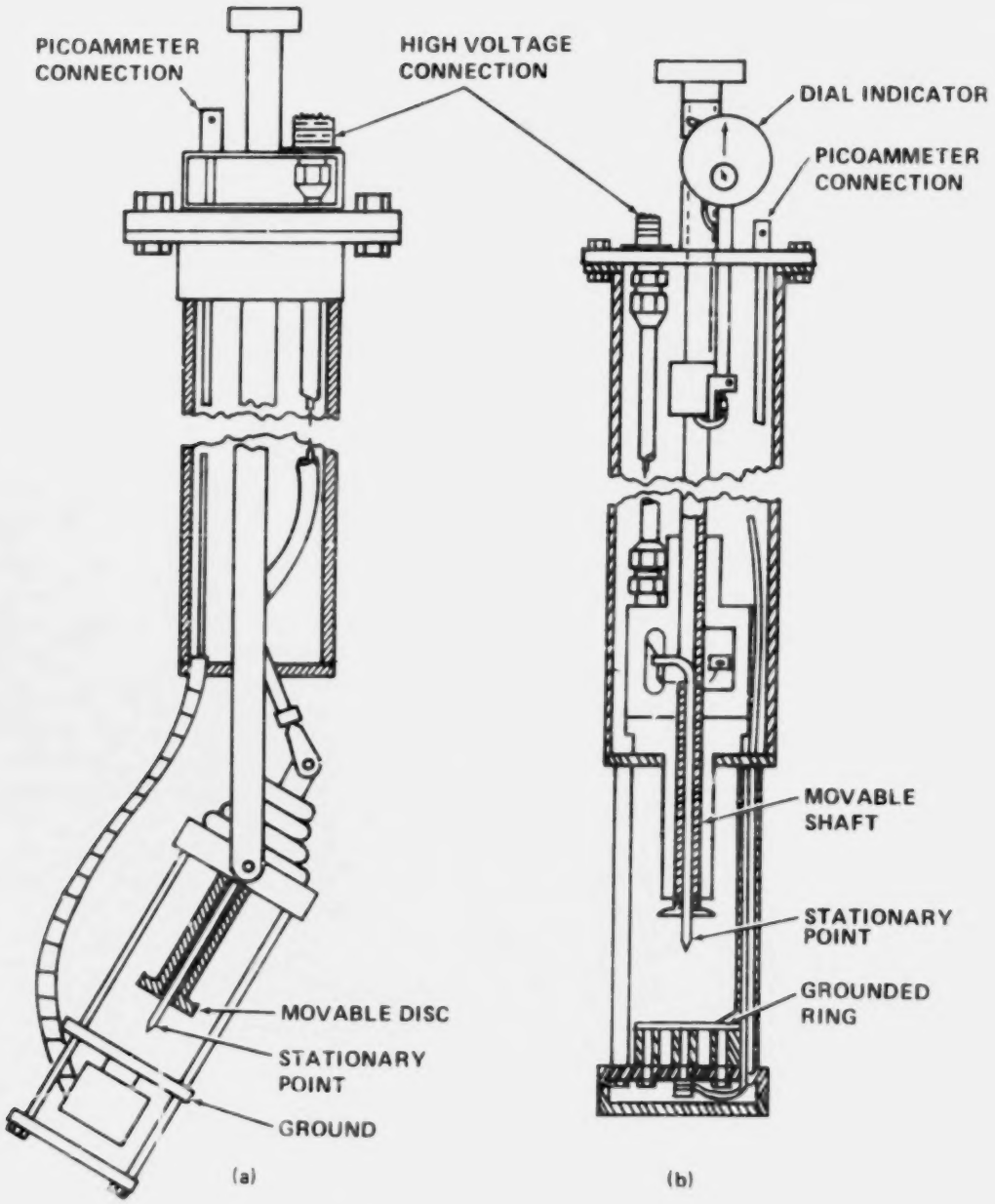

Figure 5. Point-to-plane resistivity probes equipped for thickness measurement.

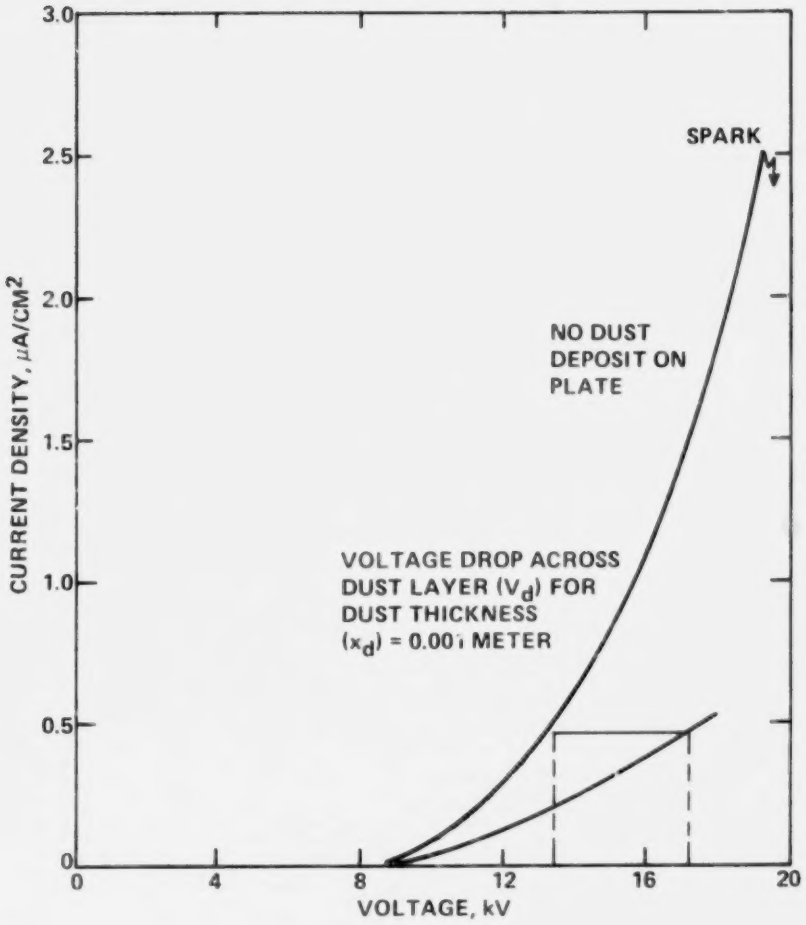

Figure 6. Typical voltage-current relationships for point-to-plane resistivity probe.

voltage. Therefore, as described in the A.S.M.E. Power Test Code No. 28 procedure, the value just prior to sparkover is reported as the resistivity.

There is considerable justification for using the value of resistivity prior to electrical breakdown as the resistivity, since it is precisely at electrical breakdown that the resistivity causes problems within the precipitator. The electrical breakdown in the dust layer in the operating precipitator either initiates electrical sparkover or reverse ionization (back corona) when the resistivity is the factor limiting precipitator behavior. If neither of these events occurs, the dust layer merely represents an additional voltage drop to the precipitator power supply.

Even though there are many similarities between the operation of the point-to-plane device and a full-scale precipitator, several problems also exist. The first problem encountered is the determination of the thickness of the dust layer. Some devices use a thickness measurement system built into the probe. In other devices, the instrument is withdrawn from the duct and the thickness of the layer is estimated visually by inspecting the dust layer. However, the dust layer is almost always disturbed by the air flow through the sampling port and extreme care is required to preserve the layer intact.

The advantages of utilizing the point-to-plane probe for in situ measurements are:

1. The particulate collection mechanism is the same as that in an electrostatic precipitator.

2. The dust-gas and dust-electrode interfaces are the same as those in an electrostatic precipitator.

3. The measurement electric field and current densities are comparable to those in the precipitator.

4. Flue gas conditions are preserved.

5. The values obtained for the resistivity are, in general, consistent with the electrical behavior observed in the precipitator.

6. Measurements can often be made by two different methods.

The disadvantages are:

1. The measurement of the dust layer thickness can be difficult.

2. High voltages are required for collection.

3. Considerable time is required for each test.

4. Experienced personnel are required for testing.

5. A number of measurements are required for gaining confidence in the measured value (there is considerable scatter in the data).

6. Particle size of the collected dust is not representative.

7. Sample size is small.

8. Carbon in the ash can hamper resistivity measurements.

RESISTIVITY MEASUREMENTS AT PLANT MITCHELL

Attempts were made to measure the in situ electrical resistivity of the fly ash after the air preheater during all three phases of the test program. Unfortunately, these attempts met with varying degrees of success.

The fly ash during the Phase I testing had a relatively high carbon content which caused considerable error in the measurement of the resistivity of the remainder of the particulate with the disc-to-disc, direct contact method of measurement. However, some data may be gleaned from the V-I method of measurement, as the accompanying Figures 7 and 8 illustrate. The resistivity referred to in the figures is the average of the resistivities computed at each data point indicated. These resistivities were 2.5×10^{11} ohm-cm from Test 1 and 2.1×10^{11} ohm-cm from Test 2. These were computed at significantly different field strengths and densities. The reason for the differences in these V-I curves has not been determined.

Considerably more data were collected during the Phase II testing. Again, the percentage of combustibles ran quite high; however, direct contact data could be obtained. These data are summarized in Table 2.

Some tests, such as 1, 6, and 7, may have been biased by the presence of the large percentage of carbon in the fly ash. Tests 1 through 5, conducted on the 24th, were collected while the boiler was operating at full load. The lower resistivities the next day were determined under two-thirds load conditions. From these data, the averages were computed and are presented in Table 3.

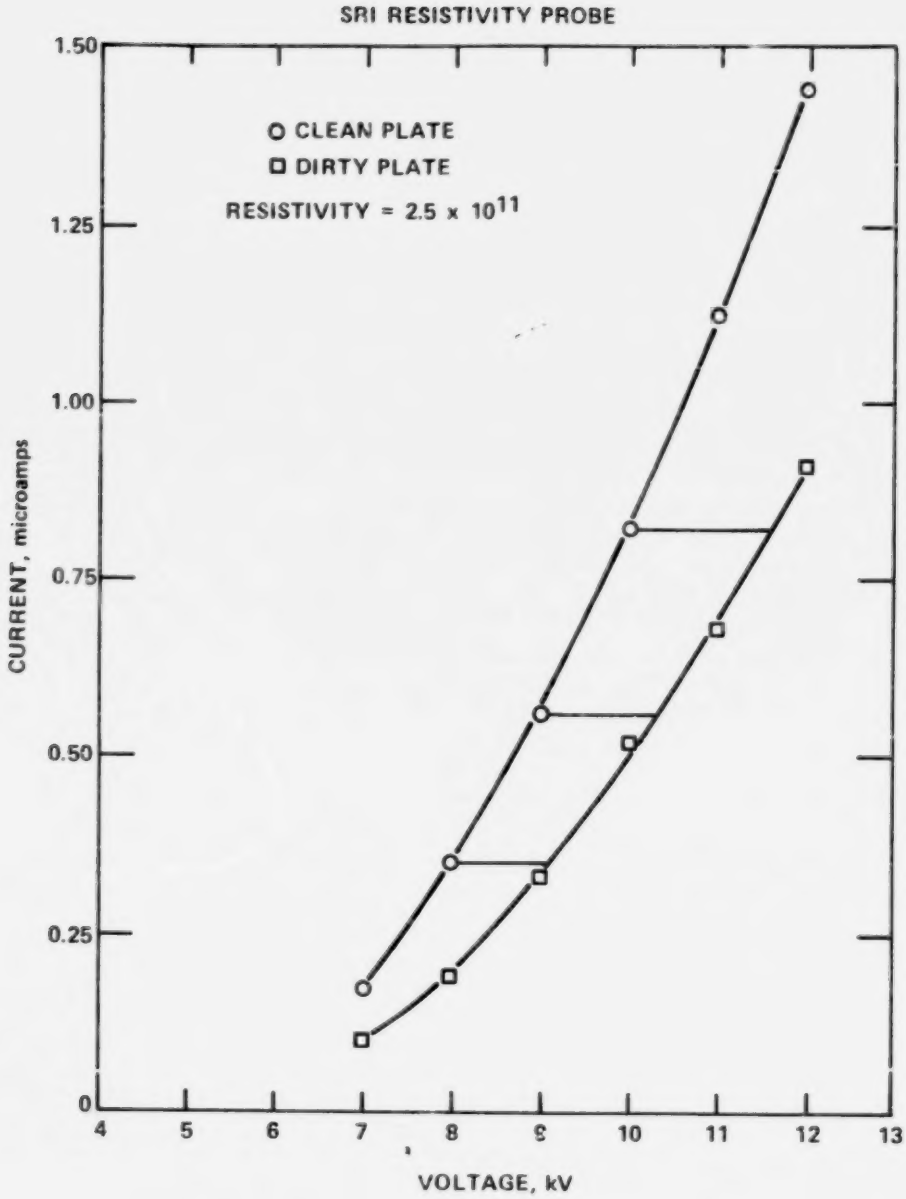

Figure 7. Voltage-current curves. Plant Mitchell full load coal Phase I, 1/25/77, Test 1.

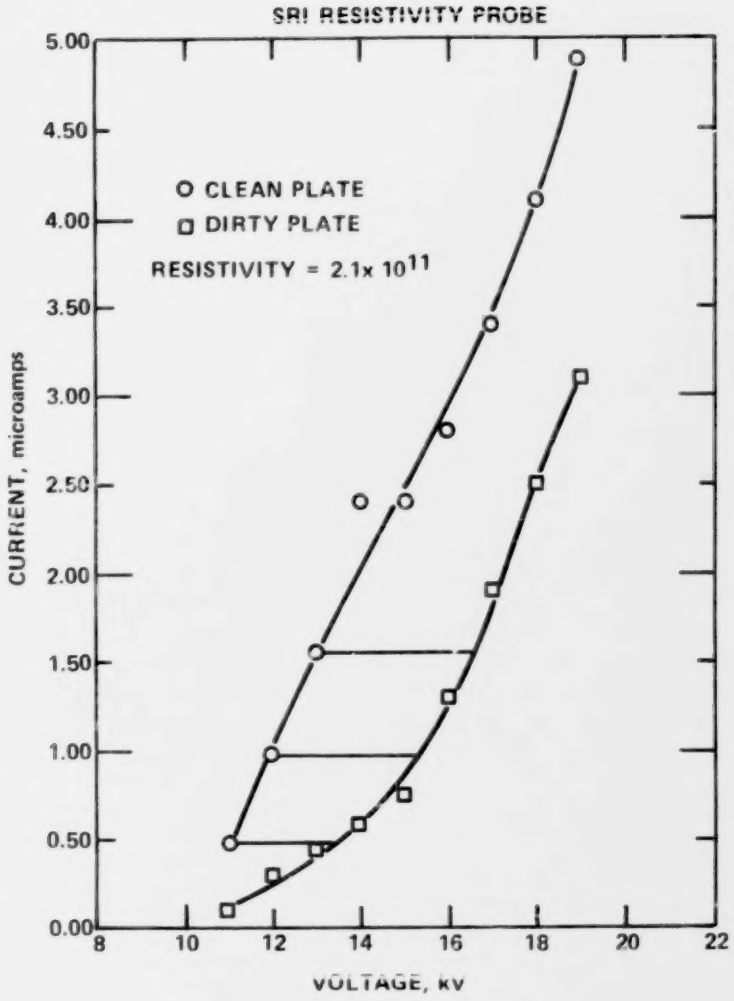

Figure 8. Voltage-current curves. Plant Mitchell full load coal Phase I, 1/25/77, Test 2.

TABLE 2. RESISTIVITY DATA—PHASE II TESTS

Test No.	Date	Temperature, °C (°F)	Resistivity, V-I method, ohm-cm	Resistivity, direct contact, ohm-cm
1	5/24	143 (290)	9.0×10^{10}	3.5×10^{7}
2	5/24	138 (280)	2.8×10^{11}	2.4×10^{11}
3	5/24	155 (311)	1.3×10^{11}	1.0×10^{11}
4	5/24	138 (280)	1.7×10^{11}	1.9×10^{11}
5	5/24	154 (309)	2.4×10^{11}	1.3×10^{11}
6	5/25	131 (268)	4.0×10^{10}	1.5×10^{6}
7	5/25	145 (293)	1.9×10^{10}	1.6×10^{8}
8	5/25	132 (270)	1.3×10^{11}	6.6×10^{10}
9	5/25	132 (270)	6.5×10^{10}	7.5×10^{9}
10	5/25	137 (278)	4.4×10^{10}	4.8×10^{9}

TABLE 3. AVERAGE RESISTIVITIES—PLANT MITCHELL PHASE II

Condition	V-I	Direct contact
Full load, Tests 1 through 5	1.8×10^{11}	1.3×10^{11}
Full load, without Test No. 1	2.1×10^{11}	1.6×10^{11}
Two-thirds load, Tests 6 through 10	6.1×10^{10}	1.6×10^{10}
Two-thirds load, without Tests 6 and 7	8.0×10^{10}	2.6×10^{10}

Phase III testing was conducted by burning the SRC. The extremely high carbon content of the ash made any sort of determination of resistivity with the in situ point-plane probe virtually impossible.

ELECTRIC POWER SET VOLTAGE-CURRENT CURVES

Data were collected during Phases II and III by recording the electrical power set's (TR's) secondary voltage versus secondary current relationships. The method of collecting these data and background information is outlined below. Actual curves and waveforms are reported in subsequent paragraphs.

Background

The electrical equivalent circuit of a precipitator is shown in Figure 9,[3] where

V = voltage applied in volts
I = total conventional current flow in amperes
C_P = equivalent precipitator capacitance in farads
R_G = effective resistance of the interelectrode gap in ohms
C_D = effective capacitance of the dust layer in farads
R_D = effective resistance of the dust layer in ohms.

The voltage normally applied to a precipitator is either half-wave or full-wave rectified 60 Hz ac. Neglecting for a moment the effects of C_D and R_D, the capacitor, C_p, charges on the increasing portion of the voltage waveform and discharges on the decreasing portion. The current from the discharging capacitance flows through the resistance R_G tending to maintain the peak voltage applied. There is an exponential decay of this voltage dependent on the time constant of the R_GC_p circuit. This time constant is given by:[4]

$$T = R_GC_p \text{ seconds}$$

where: T = time in seconds for the waveform to decrease to approximately 37% of its peak value after the voltage is removed

R_G = equivalent resistance of the interelectrode region in ohms

C_p = equivalent capacitance of the electrode system in farads.

The current, I, will flow in the return leg of the circuit only during the charging of the capacitor. During the remainder of the cycle, the current supplied to R_G is the discharge current from C_p. These relationships are shown in Figure 10. In this example T is assumed to be greater than 8 msec or one-half cycle of the line voltage.

---

3. Oglesby, S., Jr., and Grady B. Nichols. A Manual of Electrostatic Precipitation Technology Part 1—Fundamentals. NTIS PB 196 380, The National Air Pollution Control Administration, Cincinnati, Ohio, 1970, p. 251.

4. Oglesby, S., Jr., and Grady B. Nichols. A Manual of Electrostatic Precipitation Technology Part 1—Fundamentals. NTIS PB 196 380, The National Air Pollution Control Administration, Cincinnati, Ohio, 1970, p. 254.

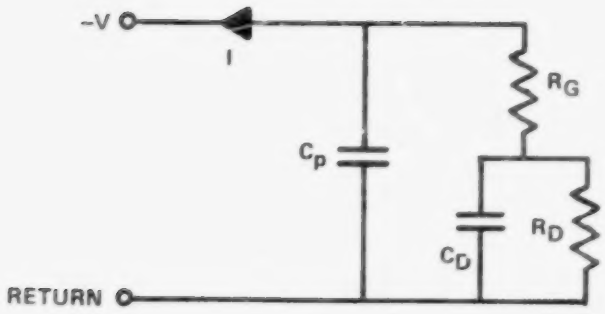

Figure 9. Electrical equivalent circuit of a precipitator electrode system with a dust layer.

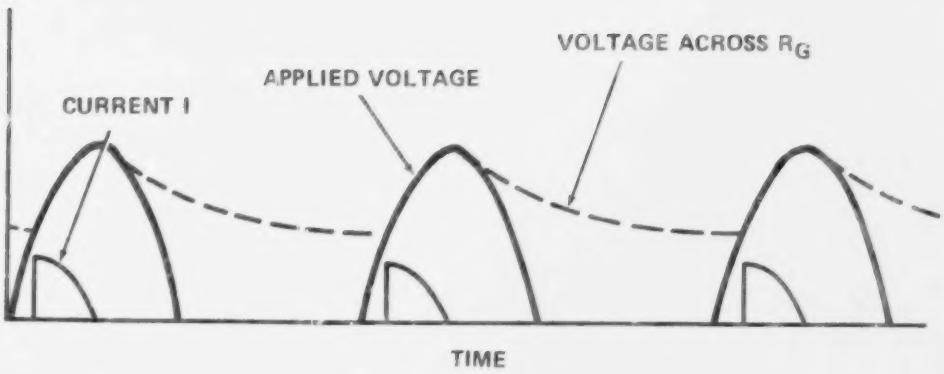

Figure 10. Voltage-current relationship in an ideal capacitor resistor parallel combination.

Normally the effective impedance presented by the parallel combination of C_D and R_D is negligible compared to the impedance of R_G. Thus, the time domain response of the precipitator is determined by the combination of C_p and R_G. However, this is not true when the dust layer is in a breakdown condition and possibly exhibiting back corona. The breakdown may effectively short out the dust layer and a portion of R_G thereby reducing the time constant, T, and increasing the current I. This change in time constant may be monitored on an oscilloscopic presentation of the voltage waveform and used to support evidence that breakdown of the dust layer is occurring.

The voltages and currents in a precipitator are most often measured by the installed power set instrumentation as root-mean-square (RMS) or effective values. The capacitances and resistances vary slowly with time so that the equivalent circuit of a precipitator in normal operation can be approximated as a pure resistance across the terminals of a dc source. The voltage-current relationship is simply $V = RI$ where R is the effective value of the resistance in ohms, V is in RMS volts, and I is in RMS amperes. An actual precipitator departs from the ideal in that R is a nonlinear function of the current. The graphical presentation of precipitator voltage versus secondary current is not the straight line as generated with an ohmic resistance but generally curved, and referred to as a V-I curve.

V-I Curve Measurement Techniques

The measurement of V-I curves at Plant Mitchell entailed the direct measurement of power set secondary voltages and currents. Today, most precipitator manufacturers install secondary kV and current (milliamp) meters on each TR set. These readings may be used directly when taking V-I data. However, in the instances when there is no secondary kV meter, as occurred with ESP No. 1, or when greater accuracy is required, calibration with known voltage dividers and an accurate voltmeter may be necessary.

The secondary voltage meter calibration involves inserting a known resistive voltage divider in parallel across the high-voltage bus section of the precipitator and taking comparative readings with the dc kV meter installed on the power set controller. The installation of this device is shown schematically at point No. 1 in Figure 11.

Figure 12 is a facsimile of a data sheet used to collect data from which voltage current relationships may be plotted. In the general heading, information is recorded which will identify the test, the power supply (TR Set), the plate area fed by the power set, and the determined calibration factors for the voltage and current. Data are taken as the manual set control is gradually increased until some current flow is detected. This is recorded as the corona starting voltage. Subsequent points are

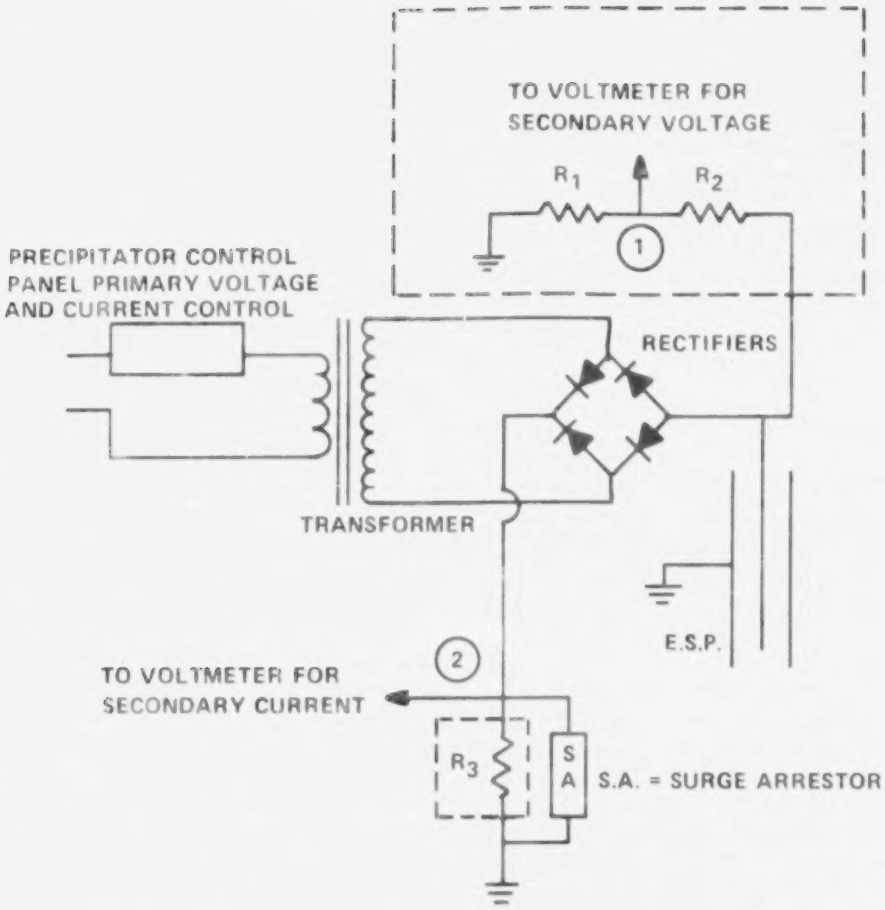

Figure 11. Voltage divider network for measuring precipitator secondary voltages.

POWER SET
VOLTAGE-CURRENT CURVE DATA SHEET

DATE/TIME_____ T/R SET NO. _____ COLLECTING AREA _ _____

VOLTAGE DIV. MULT. _____

T/R SET DCMA CORRECTION_____

PRIMARY VOLTS	PRIMARY AMPS	DCKV T/R SET METER	DCMA T/R SET METER	SPARK RATE	DCMA CORR.	DC VOLTS VOLTAGE DIV.	DCKV CORR.	$\mu A/ft^2$	NA/cm^2	TERMINAL POINT DETERMINED BY (CIRCLE ONE)
										1. SPARKING
										2. SEC. CURRENT LIMIT
										3. SEC. VOLTAGE LIMIT
										4. OTHER _____
										COMMENTS:

Figure 12. Sample V-I curve data sheet.

taken by increasing the control for some increment of current and recording the meter readings at that point. Readings are taken until some limiting factor is reached. This factor is recorded on the right-hand side of the data sheet and is usually excessive sparking or a current or voltage limitation of the power set.

The columns usually completed for each point include the primary voltage and current, the secondary kV meter on the TR set, the secondary current from the TR set, the spark rate, and the dc voltage from the voltage divider. At a later time the DCMA correction factor is applied to the TR set meter reading and the corrected DCMA column is completed.* The DCKV CORR column is completed by multiplying the dc Voltage DIV. column by the voltage divider multiplier. The last two columns are completed by dividing the DCMA CORR. by the appropriate collecting area in square feet or square centimeters and applying a multiplicative factor of 10^{-3}. A plot is then made on linear graph paper of the DCKV CORR. versus $\mu A/ft^2$ or nA/cm^2, depending on the experimental requirement.

Electrical Energization

The effluent gas from Boiler No. 1 passes through ESP No. 1 and combines with the gas from ESP No. 2 to pass through a third precipitator, for the purposes of the report, called ESP No. 3. The two electric sets for ESP Nos. 1 and 2 are housed in a single building on the ground between the two precipitators. The high voltage is switchable so that TR Set No. 1 may feed each inlet field in dual half-wave operation or it may feed the inlet and outlet field of ESP No. 1 also in a dual half-wave configuration. Testing was conducted utilizing the second aforementioned option. ESP No. 3 had two TR's, one each for the inlet and outlet fields in a full-wave configuration. The controls were located some 60 m (200 ft) away from the penthouse above the precipitator which contained the transformer-rectifier sets.

Voltage dividers were installed on the high voltage busses of ESP No. 1 for each V-I curve due to the nonexistence of kV meters. The kV meters and voltage dividers were installed during Phase III for calibration purposes in accordance with the preceding paragraphs. Photographs of the voltage waveforms were taken with an oscilloscope camera monitoring the low level signal from the voltage dividers.

---

* On a dual half-wave installation where the voltage is measured on one independent HV bus but the current is the sum of both sections, the secondary current must also be multiplied by the ratio of the plate area of the section under test to the total plate area in order to approximate the secondary current in that power supply leg.

Figure 13 is a plot of the V-I curves from ESP No. 1, inlet and outlet fields, for both full-load coal and SRC. As the curves on ESP No. 1 were taken, the inlet and outlet fields had essentially the same voltages applied. There were no independent voltage controls on the inlet and outlet fields. Normally all fields upstream of the field under test are at their operating points while a V-I curve is being taken. Thus, there may be some ambiguity in the lower portion of the curve for the outlet field. Figure 14 shows the curves from ESP No. 3. These curves do not show the corona initiation point due to a design limitation on the mechanical voltage adjustment.

The large shift directly to the right in the curves from ESP No. 1 and the relatively smaller shift for the curves from ESP No. 3 may be explained by the following arguments if the resistivity of the dust were in the typical ranges found in the fly ash from coal fired boilers. (1) Space charge current suppression would be likely if the particle size distributions show a large increase in the number of smaller particles, or (2) some buildup on the discharge electrodes from the time the precipitator was cleaned and coal burned, and the burning of the SRC. However, these arguments alone could not explain the large shift in voltage which has occurred in ESP No. 1. A third, most likely possibility results from the fact that the fly ash from the SRC had an extremely low resistivity due to the excessively high carbon content.

Bickelhaupt[5] has shown that in the range of temperature at this installation (about 150°C), surface conduction is the primary conduction component in the dust layer. The mechanism of this conduction consists of the migration of alkali metal ions toward the negative electrode. The resistivity of the dust determines the ease of this migration.

Gooch and Piulle[6] indicate that the electrical force tending to hold a dust layer to the surface of the collection electrode may, in fact, be negative, thus actually repelling the dust layer. This can occur with very low resistivity dusts as in the case of the fly ash from the SRC.

---

5. Bickelhaupt, R. E. "Surface Resistivity and the Chemical Composition of Fly Ash". APCA Journal, Vol. 25, No. 2. February 1975, pp. 148-152

6. Gooch, J. P., and W. Piulle. "Studies of Particle Reentrainment Resulting from Electrode Rapping". June 1977 Denver Proceedings.

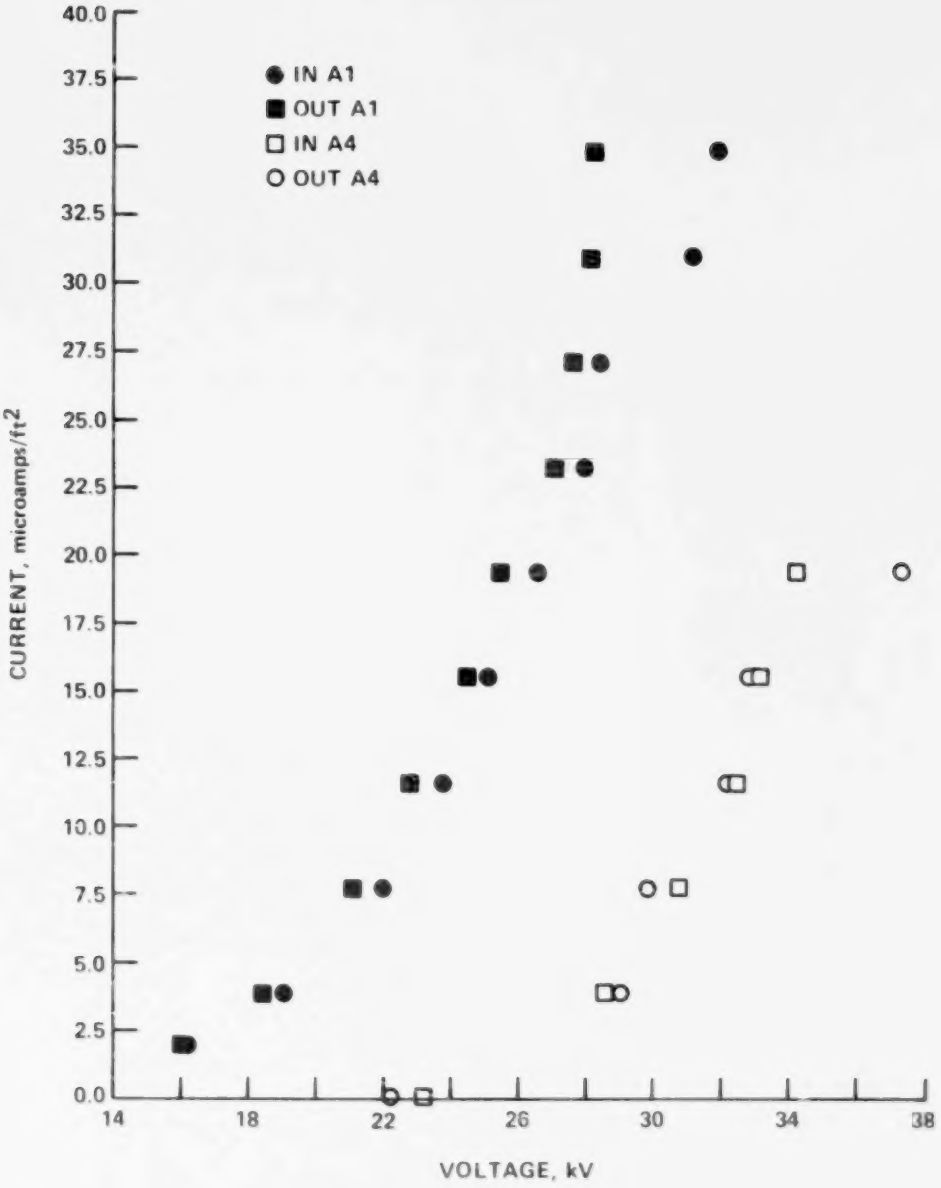

Figure 13. Voltage-current curves.
ESP No. 1 full load coal 5/24/77 - In A1 and Out A1.
ESP No. 1 full load SRC 6/22/77 - In A4 and Out A4.

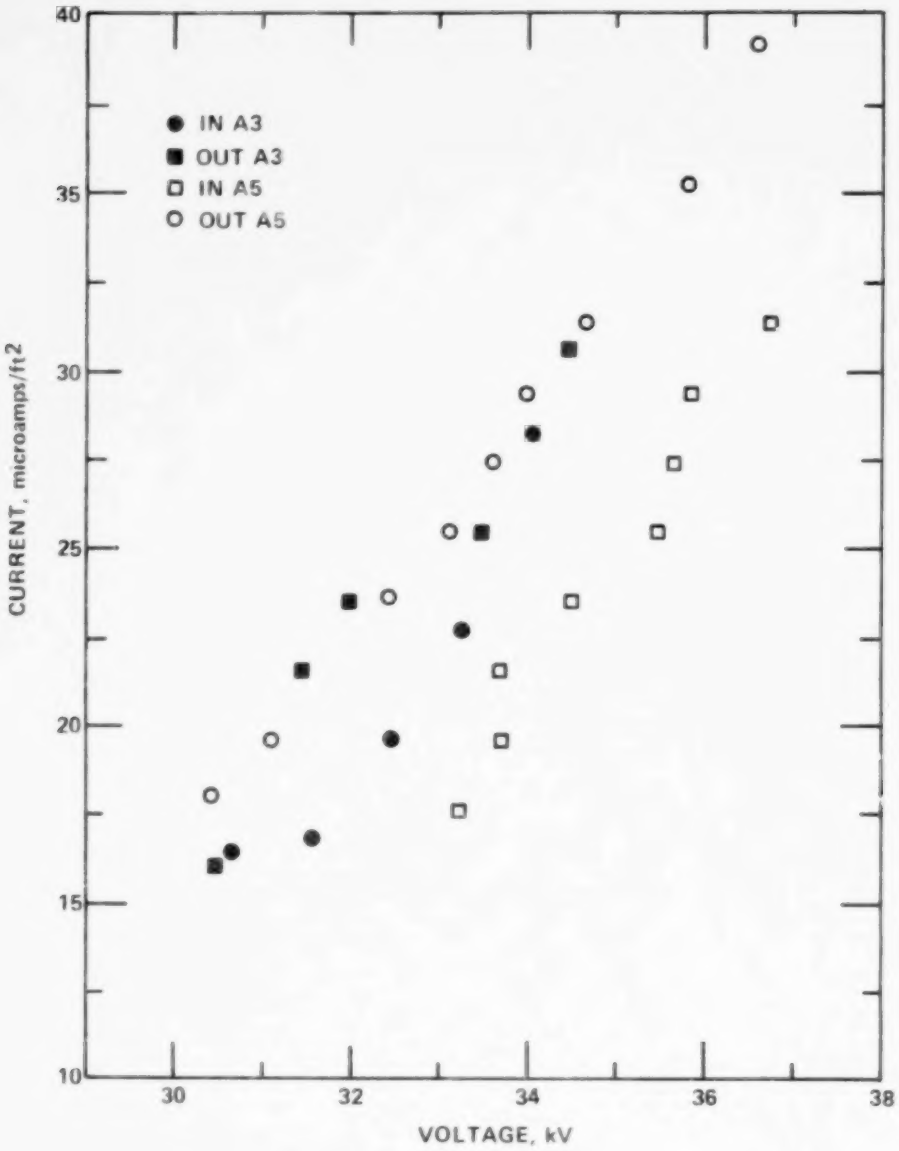

Figure 14. Voltage-current curves.
ESP No. 3 full load coal 6/8/77 - In A3 and Out A3.
ESP No. 3 full load SRC 6/22/77 - In A5 and Out A5.

From the above discussion it may be theorized that positive charge could build up on the plates and collected dust and could be rapidly transferred to the dust particle on impact. Then this particle is repelled and reentrained in the gas stream. The presence of these positively charged particles greatly reduce the efficiency of the unit and causes a decrease in current for a given voltage. Thus, the position of the V-I curves in Figures 13 and 14 may be explained by large numbers of positively charged particles being reentrained into the gas stream.

Facts in support of this include:

1. Measured efficiency of ESP No. 1 while burning SRC was 20% average.

2. Measured carbon content of the fly ash from SRC was more than 80%.

3. ESP No. 1's collection electrodes were expanded metal plates, decreasing the area to which a particle might adhere.

4. The gas velocity in ESP No. 1 was almost four times the velocity in ESP No. 3 tending to increase the reentrainment.

5. The SCA of ESP No. 3 was five times that of ESP No. 1, which would tend to reduce the amount of current suppression.

6. The measured bulk density of the fly ash during the SRC burn was 0.2 g/cm^3, compared with usually measured bulk densities of the order of 2.0 g/cm^3, which also would tend to increase the tendency toward reentrainment.

7. The ash appeared to be nonadhesive since only those large particles trapped in the crevices of the point-plane probe were found when the power was removed from the probe and the probe withdrawn from the flue.

It is hoped the above discussion explains (1) the reason the curves are shifted to the right when burning SRC, and (2) the reason the curves on ESP No. 1 are shifted more than ESP No. 3.

Voltage Waveform Photographs

Figure 15a, b, and c are photographs of the oscilloscope presentations of the high-voltage waveforms from the precipitators under full-load conditions. Figure 15a and b are from ESP No. 1 while firing coal and SRC, respectively. Figure 15c is from

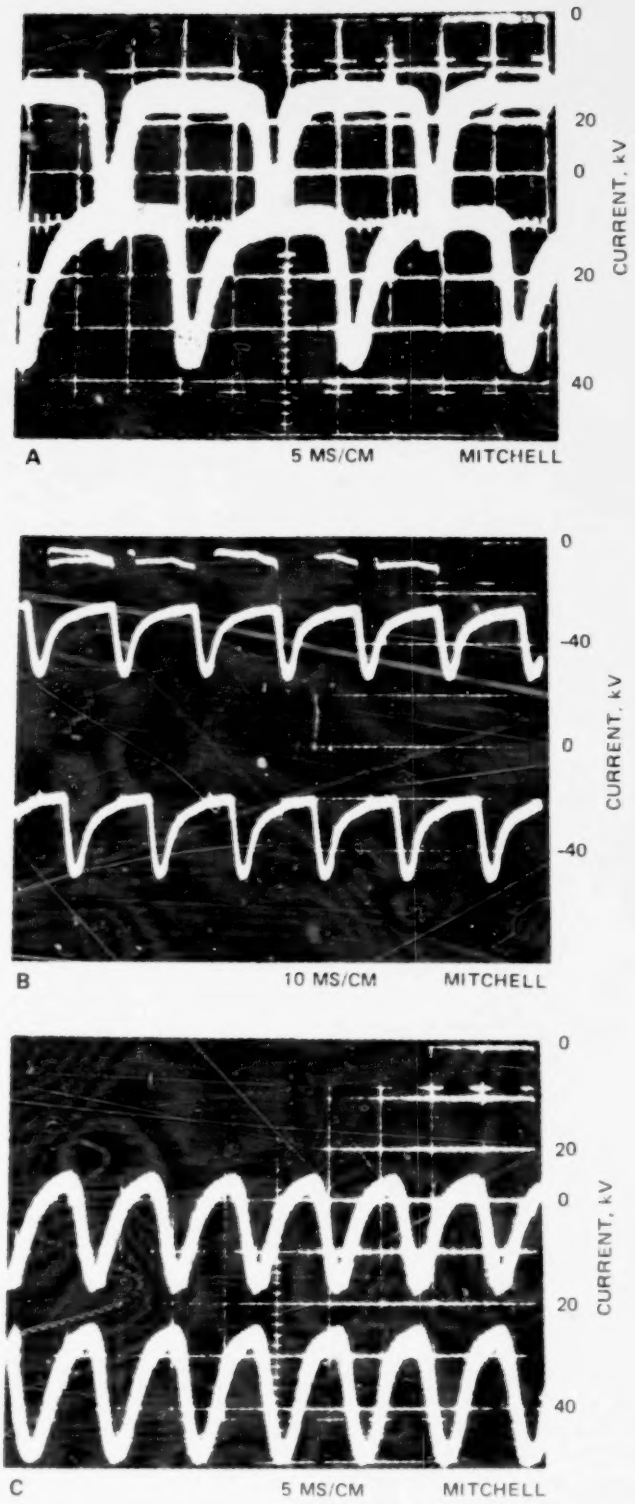

a. ESP No. 1 full load coal.
b. ESP No. 1 full load SRC.
c. ESP No. 3 full load SRC.

Figure 15. Voltage waveforms applied to the precipitators at Plant Mitchell.

ESP No. 3 during SRC operation. The top trace of each photograph is the inlet field; the bottom trace, the outlet. The zero reference for the top trace on all the photographs is the upper horizontal line of the graticule marked with a zero in the right hand margin. The zero near the center of the photograph in the right-hand margin is the zero reference for the lower trace. The horizontal time per division is given in the lower margin.

In observing the photographs it should be noted that these are negative voltages and no polarity inversion has been introduced. Therefore, the top of the waveform, as viewed, is the minimum magnitude of the negative voltage. This minimum normally coincides with the corona starting voltage. However, in cases where the resistivity of the dust layer is high enough to generate a back corona, the minimum may approach zero more closely; that is, it may fall below the corona initiation voltage.[7]

There is a noticeable change in the top of the voltage waveform in Figure 15a which corresponds to a corona starting voltage in the range of 10 to 15 kV, as compared to Figure 15b where the corona starting voltage is now in the range of 22 to 28 kV. This was also seen in the V-I curves in Figure 13 as a shift to the right and was discussed at that time. Figure 15c shows the full wave rectified waveforms applied to ESP No. 3 during the Phase III tests. Visual inspection of the three waveforms show no transition of the waveforms below the corona start, and a relatively short delay time, both supportive of the assumption that the resistivity of the dust is not so high as to be detrimental to the electrical operation.

From the resistivity, V-I curves, and voltage waveform data presented, it can be concluded that during the Phase II burn, resistivity of the dust did not appear to limit the precipitator performance. However, in the Phase III burn the extremely low dust resistivity had a disastrous effect on the operation of the precipitators, as exemplified by the reduced efficiency of ESP No. 1 from 76 to 20%.

---

7. Nichols, Grady B. "Techniques for Measuring Fly Ash Resistivity", EPA Report No. 650/2-74-079, US Environmental Protection Agency, p. 326.

SECTION 5*

COLLECTION OF SAMPLES FOR CHEMICAL ANALYSIS

PROCEDURES

This section describes the sampling program conducted with the Source Assessment Sampling System during the burning of both regular coal (Phase II) and solvent refined coal (Phase III). Samples were collected primarily at the inlet and outlet of ESP No. 1 under full- (21 MW), medium- (14 MW), and low- (7 MW) load conditions. Two additional samples were obtained at the outlet of ESP No. 3, with Unit No. 2 offline and Unit No. 1 at 21 MW, during burns with each type of coal.

Two types of gasket and O-ring material—Viton and Teflon—were used during the Phase II test program. Two sets of runs were made, under supposedly identical plant operating conditions, to assess the physical and chemical integrity of Viton against that of Teflon.

All samples were processed and combined according to the protocol given in IERL-RTP Procedures Manual: Level I Environmental Assessment, June 1976, or the April 24, 1977, amendment to that manual. The samples were then shipped to Hittman Associates, Inc., along with coal samples and SASS train data sheets. The results of the analyses of these samples will be found in a separate report prepared by Hittman Associates, Inc., under Contract No. 68-02-2162.

The SASS train supplied by the Environmental Protection Agency was cleaned and rechecked in our laboratory and found to perform satisfactorily. A spare filter holder, Teflon and Viton gaskets and O-rings, and impinger bottles were obtained from the manufacturer, the Aerotherm Division of Acurex, Inc. A later part of this section is devoted to observations on the performance of the SASS train during the field tests.

---

* This section was prepared by Walter R. Dickson, Senior Chemist, and William J. Barrett, Head, Analytical and Physical Chemistry Division, Southern Research Institute.

Approximately 3.5 kg of XAD-2 resin was cleaned according to a modification of the Level I procedure recommended by Dr. Phillip L. Levins of Arthur D. Little, Inc. The modification consisted of extracting the resin for 24 hr with methylene chloride instead of the usual diethyl ether and pentane. No problems were experienced during the lengthy cleanup procedure. The cleaned resin contained 8 μg/150 g of extractable organic material, as determined by gas chromatography with flame ionization detection, corresponding to a concentration of 0.2 $\mu g/m^3$ for a normal SASS train run of 5 hr at 0.11 m^3/min (4 ft^3/min).

Samples were collected at three locations during both phases of the test program: at the inlet and outlet of ESP No. 1, and at the outlet of ESP No. 3. Since the flue gas from ESP No. 2 was combined with that from ESP No. 1 prior to entering ESP No. 3, Unit No. 2 was taken offline for the ESP No. 3 tests.

During Phase II it was necessary to delay the start of the SASS train runs at ESP No. 1 for about 2 hr until a port was cleared by other test crews. Additional sampling ports were installed during the interval between Phases II and III to eliminate this problem. At each sampling location the SASS probe was positioned in the duct in a region representative of the average velocity across the duct at that particular port. No attempt was made to traverse the duct during any of the runs.

SAMPLES COLLECTED DURING PHASE II

Table 4 presents a compilation of data from the SASS train runs during the Phase II test program. In most runs considerable difficulty was experienced in maintaining an 0.11 m^3/min (4 ft^3/min) sampling rate at either the inlet or outlet of ESP No. 1 due to clogging of the particulate filter. Because of restrictions imposed by plant operations on the time available for sample collection and because approximately 20 to 30 min was required to replace filter holders and reheat the oven to 200°C (400°F), it was impossible to change filters as often as was desired. Since the grain loading at the outlet of ESP No. 3 was very low, no significant pressure drop was encountered, even though nearly 80% of the particulate appeared to be less than 1 μm in size.

A black stain was observed in the upper region of the organic module on all runs. This stain was apparently insoluble in the methylene chloride/methanol rinse solution and could only be partially removed by vigorous scrubbing with a nylon brush. The aqueous condensate collected by the organic module was always light green in color. Immediately following the termination of each run, the condensate—usually 700 to 1000 ml—was extracted three times with about 100 ml of methylene chloride. The color remained in the aqueous phase in all samples.

TABLE 4. DATA FROM RUNS WITH REGULAR COAL (PHASE II)

Date	Sampling location	Gasket material	Load condition, MW	Volume sampled, m³ (dry)	Average sampling rate, m³/min (dry)	Total particulate collected, g	Weight % of particulate				Particulate concn, g/m³ (dry)
							Cyclone				
							10 μm	3 μm	1 μm	Filters	
5/25	Outlet ESP No. 1	Teflon	14	29.6	0.0974	14.67	37.3	29.0	28.1	5.5	0.494
5/26	Outlet ESP No. 1	Teflon	7	*							
5/27	Outlet ESP No. 1	Teflon	21	30.5	0.1050	32.61	44.1	24.0	24.0	7.9	1.071
5/28	Inlet ESP No. 1	Teflon	21	29.0†	0.0994	132.81	48.4	37.3	11.7	2.6	4.576
5/29	Inlet ESP No. 1	Viton	14	30.0	0.1025	90.50	42.5	39.0	15.8	2.7	3.020
5/30	Outlet ESP No. 1	Viton	14	30.0‡	0.1039	28.51	51.5	25.6	16.4	6.6	0.954
5/31	Outlet ESP No. 1	Viton	7	27.6‡	0.1062	8.08	38.6	33.7	24.6	3.0	0.295
6/2	Inlet ESP No. 1	Viton	7	26.2‡	0.1048	154.39	49.9	34.4	12.3	3.4	5.880
6/5	Outlet ESP No. 3	Viton	21	35.1§	0.1110	0.076	4.5	3.3	14.6	77.7	§
6/6	Outlet ESP No. 3	Teflon	21	18.6#	0.1113	0.052	4.7	0.2	15.2	80.4	0.002

* The fire went out in the boiler during the early stages of this run. The SASS test was aborted.

† The fire again went out in the boiler. The unit was restarted on fuel oil without notifying us in time, thus this sample was contaminated.

‡ These tests were terminated early because the plant needed to go on full load because of a power shortage.

§ The probe nozzle was not facing in the direction of the gas flow during 75% of the run.

This test was terminated early when Unit No. 2 was brought on line because of a power shortage.

The appearance of the impinger solutions varied somewhat from run to run. The peroxide impinger was clear while the first and second silver nitrate/ammonium persulfate impingers were either clear or amber in color with fine black particles generally present in the first impinger and a small amount of a white agglomerated material in the second impinger.

Since the SASS train data represent only a single point sample at each location, a critical evaluation of precipitator performance, particle-size distribution, and mass loading would be presumptuous. The results do suggest, however, that ESP No. 1 was relatively inefficient, but that ESP No. 3 performed well. The particulate not collected by ESP No. 3 was predominantly less than 1 μm in size while that particulate passing through ESP No. 1 was considerably larger.

SAMPLES COLLECTED DURING PHASE III

The results obtained from the SASS train runs during the burning of solvent refined coal are given in Table 5. Severe pressure drops were encountered after about 10 min of sampling at both the inlet and outlet of ESP No. 1, but not at ESP No. 3. Obviously, filter changes could not be made this often and still complete a test run in a reasonable length of time. Therefore, filters were changed only every 35 to 40 min despite the fact that the 0.11 m^3/min (4 ft^3/min) sampling rate could not be maintained over this sampling period.

The data suggest that a proportionately greater fraction of small particles were produced during the combustion of the solvent refined coal than from regular coal. Two factors could, however, invalidate this conclusion: a lower average sampling velocity through the cyclones, and an ash that appeared to have a bulk density considerably less than the ash from regular coal.

The black stains found on the upper section of the organic module during the burning of regular coal were observed only on those runs at the outlet of ESP No. 3 for the Phase III series. On the second of these runs a narrow ring of green crystals was apparent on the wall of the inner cooler where the hot gas impinged on the cold surface.

No significant difference in the appearance of the impinger solutions was obvious between Phase II and Phase III samples.

COMMENTS ON OPERATION OF THE SASS TRAIN

Both Teflon and Viton gaskets were used during the Phase II test program. Teflon gaskets have a tendency to leak, especially after having been used before, and considerable

TABLE 5. DATA FROM RUNS WITH SOLVENT REFINED COAL (PHASE III)*

Date	Sampling location	Load condition, MW	Volume sampling, m^3 (dry)	Average sampling rate, m^3/min (dry)	Total particulate collected, g	Weight % of particulate				Particulate concn, g/m^3 (dry)
						Cyclone				
						10 µm	3 µm	1 µm	Filters	
6/13	Outlet ESP No. 1	21	28.77	0.0960	24.02	54.3	19.7	1.6	24.4	0.830
6/14	Outlet ESP No. 1	14	28.60	0.0932	30.64	57.2	19.0	1.0	22.8	1.046
6/15	Outlet ESP No. 1	7	28.26+	0.1019	15.68	44.5	17.2	3.0	35.4	0.551
6/16	Outlet ESP No. 1	21	28.46‡	0.0943	23.93	53.7	12.4	1.3	32.7	0.837
6/17	Inlet ESP No. 1	21	30.04‡	0.0946	41.75	62.2	12.1	0.8	24.9	1.382
6/18	Inlet ESP No. 1	7	29.87	0.0951	33.71	47.7	14.2	1.0	37.2	1.123
6/19	Outlet ESP No. 1	7	30.16	0.0980	15.62	44.7	20.4	1.7	33.3	0.501
6/20	Outlet ESP No. 1	14	§‖							
6/21	Inlet ESP No. 1	14	#							
6/22	Outlet ESP No. 3	21	32.22	0.1073	0.186	3.9	1.8	2.7	91.6	0.007
6/23	Outlet ESP No. 3	21	32.85	0.1086	0.193	13.7	3.6	4.1	78.6	0.007
6/24	Outlet ESP No. 1	23.5	30.30	0.0977	18.03	41.6	26.9	1.7	40.8	0.593

* The gasket material used in all tests was Teflon.

+ This test was terminated after a near loss of fire in the boiler.

‡ Power was lost during the run, resulting in impinger solutions backing up into the organic module. All samples except the particulates were discarded.

§ Power was insufficient to run the SASS train. This run was aborted.

The plant lost a coal mill during the early part of this run and all testing was cancelled.

be expected in attaining a satisfactory leak rate check. One solution to this problem was to wrap all outer cyclone, filter, and organic module flanges with Teflon tape before applying the clamps. By following this procedure an acceptable leak rate test was obtained with the same gaskets on 13 sampling runs.

Viton gaskets provided an excellent seal for the five runs in which they were used, but the cyclones became increasingly more difficult to dismantle with each test. Finally, the flanges had to be pried apart. The Viton appeared to be partially bonded to the metal and was physically distorted. The same problem did not occur with the seals in the organic module, which were, of course, not subjected to the 200°C (400°F) oven temperature. Although the flange clamps were loosened appreciably from the tension normally applied to the Teflon gaskets, there is a possibility that the Viton gaskets may still have been overly compressed. However, it seems likely that the bonding problem would have been encountered on the initial runs if that were the case. Since only one set of the Viton gaskets was available, additional testing of Viton could not be conducted during this field test. Teflon gaskets, therefore, were used exclusively for the Phase III test program.

Only minor problems were experienced with the SASS train during this field test; however, some suggestions for improvements in the system seem warranted.

- At locations where a significant concentration of fine particulate is present a thimble preceding the absolute filter would reduce the number of filter changes required to maintain the desired sampling rate. A somewhat larger oven would facilitate aligning the cyclones, tightening connections, and changing filters. An auxiliary heater in the oven would also decrease the downtime following a filter change.

- The present fiberglass impinger case should be enlarged and insulated.

- The new impinger bottles, with the VMP trademark, provide such a tight fit with the Teflon heads that it was difficult to dismantle them without breaking the impinger bottles.

- The glass pour spout for the condensate bottle is extremely fragile. A Teflon Swagelok bulkhead fitting through a cap on an amber bottle would be less subject to breakage.

- The braided stainless steel transfer line from the oven to the organic module should be insulated to prevent burns to test personnel. A longer line would provide greater flexibility in setting up the system at various types of sampling locations.

REFERENCES

1. Nichols, Grady B. "Techniques for Measuring Fly Ash Resistivity", EPA Report No. 650/2-74-079, US Environmental Protection Agency, pp. 2-4.

2. White, H. J. "Resistivity Problems in Electrostatic Precipitation". J. Air Pollut. Control Assoc., 24 (4), April 1974, p. 316.

3. Oglesby, S., Jr., and Grady B. Nichols. A Manual of Electrostatic Precipitation Technology Part 1—Fundamentals. NTIS PB 196 380, The National Air Pollution Control Administration, Cincinnati, Ohio, 1970, p. 251.

4. Oglesby, S., Jr., and Grady B. Nichols. A Manual of Electrostatic Precipitation Technology Part 1—Fundamentals. NTIS PB 196 380, The National Air Pollution Control Administration, Cincinnati, Ohio, 1970, p. 254.

5. Bickelhaupt, R. E. "Surface Resistivity and the Chemical Composition of Fly Ash". APCA Journal, Vol. 25, No. 2. February 1975, pp. 148-152.

6. Gooch, J. P., and W. Piulle. "Studies of Particle Reentrainment Resulting from Electrode Rapping". June 1977 Denver Proceedings.

7. Nichols, Grady B. "Techniques for Measuring Fly Ash Resistivity", EPA Report No. 650/2-74-079, US Environmental Protection Agency, p. 326.

TECHNICAL REPORT DATA
(Please read Instructions on the reverse before completing)

1. REPORT NO.	2.	3. RECIPIENT'S ACCESSION NO.
EPA-600/7-78-129		
4. TITLE AND SUBTITLE Evaluation of Electrostatic Precipitator During SRC Combustion Tests		5. REPORT DATE July 1978 6. PERFORMING ORGANIZATION CODE
7. AUTHOR(S) Grady B. Nichols and William J. Barrett		8. PERFORMING ORGANIZATION REPORT NO.
9. PERFORMING ORGANIZATION NAME AND ADDRESS Southern Research Institute 2000 Ninth Avenue, South Birmingham, Alabama 35205		10. PROGRAM ELEMENT NO. EHE623A 11. CONTRACT/GRANT NO. 68-02-2610, Task 2
12. SPONSORING AGENCY NAME AND ADDRESS EPA, Office of Research and Development Industrial Environmental Research Laboratory Research Triangle Park, NC 27711		13. TYPE OF REPORT AND PERIOD COVERED Task Final; 4-8/77 14. SPONSORING AGENCY CODE EPA/600/13

15. SUPPLEMENTARY NOTES: IERL-RTP project officer is William J. Rhodes, Mail Drop 61, 919/541-2851.

16. ABSTRACT: The report deals with the evaluation of an electrostatic precipitator (ESP) and associated environmental factors during the burning of solvent refined coal (SRC) in a boiler at Plant Mitchell of the Georgia Power Company. The effort was part of an overall study of the use of SRC in a full-scale electric power plant. Results of a performance evaluation of the ESP are reported and interpreted. Samples of stack emissions were collected with a Source Assessment Sampling System (SASS) train for chemical analysis; results of the analysis are to be reported later.

17. KEY WORDS AND DOCUMENT ANALYSIS

a. DESCRIPTORS		b. IDENTIFIERS/OPEN ENDED TERMS	c. COSATI Field/Group	
Air Pollution	Tests	Air Pollution Control	13B	14B
Electrostatic Precipitators	Sampling	Stationary Sources		
	Electric Power Plants	Solvent Refined Coal	13I	
Combustion		Particulate	21B	10B
Coal	Flue Gases	Source Assessment Sampling System	21D	
Solvent Extraction	Dust	SASS Train	07D	11G

18. DISTRIBUTION STATEMENT	19. SECURITY CLASS (This Report)	21. NO. OF PAGES
Unlimited	Unclassified	54
	20. SECURITY CLASS (This page)	22. PRICE
	Unclassified	

EPA Form 2220-1 (9-73)